Effects of Gamma Radiation Sterilization on the Structural and Biological Properties of Decellularized Corneal Xenografts

Mohammad Mirazul Islam[a], Roholah Sharifi[a], Shamina Mamodaly[a], Rakibul Islam[b], Daniel Nahra[a], Dina B. Abusamra[a], Pui Chuen Hui[a], Yashar Adibnia[a,c], Mehdi Goulamaly[d], Eleftherios I. Paschalis[a], Andrea Cruzat[a,e], Jing Kong[d], Per H. Nilsson[b,f], Pablo Argüeso[a], Tom Eirik Mollnes[b,g,h], James Chodosh[a], Claes H. Dohlman[a], Miguel Gonzalez-Andrades[a,i,*]

[a]Massachusetts Eye and Ear and Schepens Eye Research Institute, Department of Ophthalmology, Harvard Medical School, Boston, MA, USA.
[b]Department of Immunology, Oslo University Hospital, Rikshospitalet, University of Oslo, Oslo, Norway.
[c]Yeditepe University School of Medicine, Istanbul, Turkey
[d]Department of Electrical Engineering and Computer Science, Massachusetts Institute of Technology, Cambridge, MA, USA.
[e]Department of Ophthalmology, Pontificia Universidad Católica de Chile, Santiago, Chile.
[f]Linnaeus Center for Biomaterials Chemistry, Linnaeus University, Kalmar, Sweden
[g]Research Laboratory, Nordland Hospital, Bodø, and Faculty of Health Sciences, K.G. Jebsen TREC, University of Tromsø, Norway.
[h]Centre of Molecular Inflammation Research, Norwegian University of Science and Technology, Trondheim, Norway.
[i]Maimonides Biomedical Research Institute of Cordoba (IMIBIC), Department of Ophthalmology, Reina Sofia University Hospital and University of Cordoba, Cordoba, Spain.

*Corresponding author.

Keywords: gamma radiation sterilization; decellularization; corneal transplant; recellularization; acellular porcine cornea.

Abstract: To address the shortcomings associated with corneal transplants, substantial efforts have been focused on developing new modalities such as xenotransplantion. Xenogeneic corneas are anatomically and biomechanically similar to the human cornea, yet their applications require prior decellularization to remove the antigenic components to avoid rejection. In the context of bringing decellularized corneas into clinical use, sterilization is a crucial step that determines the success of the transplantation. Well-standardized sterilization methods, such as gamma irradiation (GI), have been applied to decellularized porcine corneas (DPC) to avoid graft-associated infections in human recipients. However, little is known about the effect of GI on decellularized corneal xenografts. Here, we evaluate the effect of radiation on the ultrastructure, optical, mechanical and biological properties of gamma irradiated decellularized porcine corneas (G-DPC). Transmission electron microscopy revealed that G-DPC preserved its structural integrity. Moreover, GI did not deteriorate the optical properties of the tissue. Human complement activation products did not significantly overexpress in contact with DPC and G-DPC. Additionally, DPC were mechanically comparable with the native tissue; however, GI increased the mechanical strength as well as the tissue hydrophobicity and the resistance to enzymatical degradation. Despite of those changes, human corneal epithelial, stromal and endothelial cells, as well as hybrid neuroblastoma cells, were able to grow and differentiate on DPC and G-DPC. Thus, GI is not deleterious for the tissue and allows retention of physiological, mechanical and optical properties required for corneal transplantation.

Statement of significance:

In the context of bringing decellularized porcine corneas into clinical use, sterilization is a crucial step that determines the success of the transplantation. Well-standardized sterilization methods, such as gamma irradiation (GI), have been applied to decellularized xenografts to avoid graft-associated infections in human recipients. However, little is known about the effect of GI on decellularized corneas despite of their recent use in clinical studies. Here, we evaluate the effect of GI on the ultrastructure, optical, mechanical and biological properties of decellularized porcine corneas in order to understand its outcomes and to facilitate its clinical translation. Our results suggest that GI is not deleterious for the tissue and allows retention of physiological, mechanical and optical properties required for corneal transplantation.

Graphical abstract:

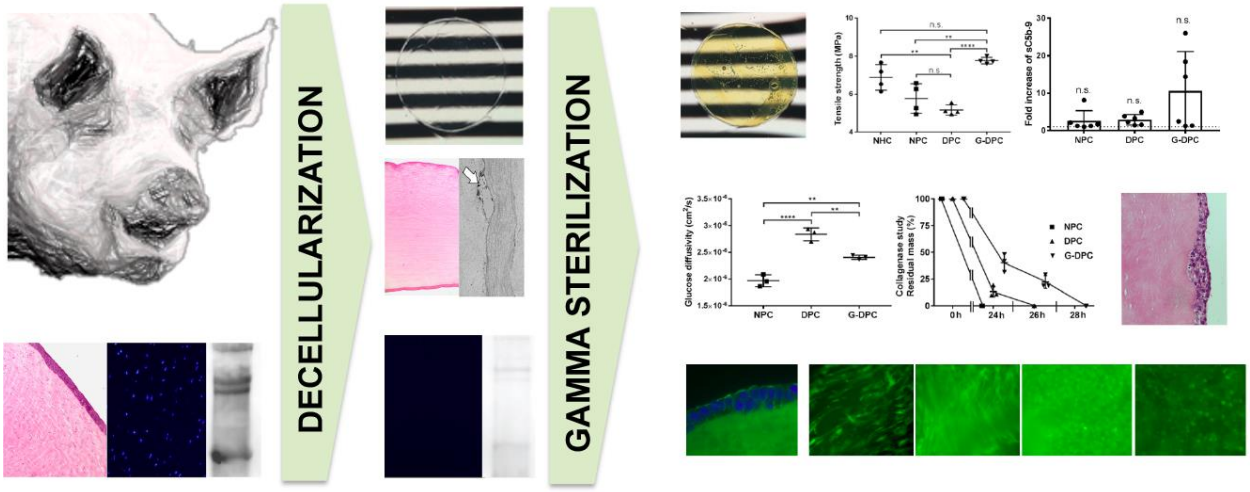

1. INTRODUCTION

Corneal diseases are one of the most important causes of blindness in the world . In severe corneal diseases, corneal transplantation is the most used and reliable treatment (Hara and Cooper, 2011; Brunette *et al.*, 2017). However, most of the world population, including 90% of the visually impaired people, live in low-income countries, where a severe shortage of donor corneas and a lack of readiness for corneal transplantation exists (Oliva *et al.*, 2012). This makes 12.7 million people worldwide waiting for a corneal transplant (Gain *et al.*, 2016). Although corneal transplantation is considered the most successful organ transplant procedure, it is associated with two major complications; immune rejection and donor-derived infections (Wong *et al.*, 2017; Vail *et al.*, 1996; Panda *et al.*, 2007; O'Day, 1989). Microbial screening and administrative cost for shipping of donor corneas make corneal allograft surgery an unaffordable treatment option for most worldwide patients (Cruzat *et al.*, 2013; Polisetti *et al.*, 2013). Thus, to compensate for the scarcity of human donor corneas and to overcome the major complications of corneal transplantation, appropriate alternatives are needed. In this context, xenografts emerge as a real possibility to replace human donor corneas. Corneas from pigs (Kissam, 1844), rabbits (1891), gibbons (Soomsawasdi B, 1964), cows (Durrani *et al.*, 1974), chickens (De Ocampo *et al.*, 1959), monkeys (De Ocampo *et al.*, 1959) and fishes (Haq, 1972) were also transplanted in the early stage of xenotransplantation in humans with very limited success. In all cases, the implant failed mainly due to host immune reaction against the graft (Larkin and Williams, 1995). Thus, complete or partial removal of donor cellular components that initiate immune reactions and activate the complement system, can be beneficial for the survival of xenografts transplanted in humans (Choi *et al.*, 2011). Furthermore, cross-species infectious diseases are another major complication of xenograft transplantation that needs to be addressed (Boneva *et al.*, 2001).

Decellularization has become an important approach to overcome these major complications in xenograft transplantation. The decellularized organs can be used as scaffolds for tissue regeneration that maintain physiological properties required to replace the target organ (Badylak, 2004). Regarding the cornea, pig (*Sus scrofa domesticus*) has been the most widely used species because of the anatomical and physiological similarities to humans (Cooper *et al.*, 2002; Lee *et al.*, 2006), including composition and structure of corneal stromal proteins (Sharifi *et al., in press)*. A number of methods have been developed to decellularize porcine corneas (Hashimoto *et al.*, 2015; Gonzalez-Andrades *et al.*, 2015). Most of these use detergents, such as sodium dodecyl sulfate (SDS), or osmotic changes with NaCl. Although detergents are cytotoxic and need to be washed out appropriately from the xenograft, they are widely used to decellularize because their use is simple and inexpensive. In our previous work, we demonstrated the efficacy of NaCl and SDS to decellularize porcine corneas (DPC) after treatment with dispase II (Gonzalez-Andrades *et al.*, 2011) and determined the decellularizing effect of benzalkonium chloride, Igepal, SDS or Triton X-100 at different concentrations and different time intervals of full corneas with corneoscleral limbus (Gonzalez-Andrades *et al.*, 2015). Moreover, detergents can be easily combined with other decellularization methods, such as NaCl, to improve the efficiency of the protocol (Zhang *et al.*, 2015). Other decellularization techniques have been described, such as high hydrostatic pressure and supercritical carbon dioxide, but they all require expensive and specialized equipments (Lynch and Ahearne, 2013; Huang *et al.*, 2017).

In the context of bringing decellularized corneas into clinical use, sterilization is a crucial step that determines the success of the transplantation. Well-standardized sterilization methods, such as gamma irradiation (GI), have been applied to the decellularized xenograft to avoid graft-associated infections in human recipients (Zhang *et al.*, 2015; Shi *et al.*, 2017). Tissue banks usually use GI for sterilization of tissues and biological substances against bacterial, viral, fungal

and prional contaminations (Miekka *et al.*, 2003; Singh *et al.*, 2016). GI has been successfully applied to human corneas. Most of patients that received a gamma irradiated human cornea showed favorable outcomes without graft rejection, loss of transparency or neovascularization (Wee *et al.*, 2015). GI also reduces the allogenicity (Stevenson *et al.*, 2012) and increases the shelf life of the sterile irradiated human corneas for more than one year at room temperature (Yoshida *et al.*, 2015; Stevenson *et al.*, 2012). However, little is known about the effect of GI on decellularized porcine corneas despite of the recent use of these xenografts in high-risk patients with infectious keratitis (Zhang *et al.*, 2015)(Shi *et al.*, 2017).

Thus, there is still a need for evaluating the effect of gamma radiation on the ultrastructure, optical, mechanical and biological properties of decellularized porcine corneas in order to understand its outcomes and to facilitate its successful translation into the clinical practice. In the present work, we optimized the decellularization of porcine corneas using SDS in distilled water (dH_2O) and sterilization with 25 kGy of GI. Afterwards, we evaluated biocompatibility and *in vitro* complement activation before and after GI. Furthermore, optical and mechanical properties were investigated as well as the feasibility of implanting this tissue in *ex vivo* models of keratoplasty and keratoprosthesis implantation. The similarity of physiological, mechanical and optical properties of human and porcine corneas (Cooper *et al.*, 2002; Lee *et al.*, 2006), including stromal protein composition (Sharifi *et al., in press),* was the rationale behind selecting porcine cornea for this study.

2. MATERIALS AND METHODS

2.1. Preparation of decellularized porcine corneas (DPC)

Fresh porcine eyes were obtained from adult pigs immediately after their death at a local slaughterhouse. After receiving the eyes, corneas were inspected with a portable slit lamp (S150, MediWorks Precision Instruments; Shanghai, China) to discard those showing any corneal damage. Selected corneas were removed from pig eyes with a 16 mm diameter trephine and washed with phosphate buffer saline (PBS). In every experiment, native porcine corneas (NPC) without further processing for decellularization were used as control. For decellularization, corneas were placed in a 6-well plate, facing epithelial side down (1 cornea per well). 0.1% SDS (Applied Biosystems, CA, USA) buffer in dH_2O was added to the wells. After 72 hours, SDS was replaced by PBS and maintained for 48 hours. All the solutions were 5 ml in volume and changed every 24 hours. NPC in dH_2O for 72 hours served as a secondary control of this study. Finally, DPC were immersed into 100% glycerol (5 ml) to dehydrate and kept there at room temperature without shaking until further use. The complete decellularization process was carried out under continuous shaking (70 rpm) at room temperature.

2.2. Evaluation of decellularization process

For histological evaluation, DPC were fixed in 4% paraformaldehyde, dehydrated in increasing concentrations of ethanol (70%, 96%, 100%) for 30 minutes at each concentration. Then the tissues were immersed twice in xylene for 30 minutes and then kept in liquid paraffin for 30 minutes. The paraffin-embedded sections were cut to 6 μm thickness with a microtome and stained for histology. Staining with hematoxylin for 2 minutes and eosin for 1 minute (H&E, Hematoxylin Stain, Fisher Chemical, NJ, USA and Eosin Y, Fisher Chemical) was done for histological examination. Staining with 1% Alcian blue (AB, Electron Microscopy Science, PA, USA) for 30 min was done to visualize the glycosaminoglycans (GAG) accumulation (Yuan *et al.*, 2016). Staining with Periodic acid–Schiff (PAS, Fisher Chemical) for 15 minutes together

with counterstain of hematoxylin for 1 minute was done to detect the presence of polysaccharides, principally glycogen (O'Rahilly and Meyer, 1960).

To determine the decellularization efficiency, the number and area of remaining nuclei and nuclear debris in NPC and DPC (3 corneas per group) were quantified by using 4,6-diamidino-2-phenylindole (DAPI) staining (VectaShield mounting medium containing DAPI - Vector Laboratories, Inc., CA, USA) on deparaffinized tissue sections (3 sections per cornea were analyzed) and the percentage of cell removal was determined. To capture representative pictures of the entire corneal stroma of every sample, we devised a specific pattern of photography that ran from anterior to posterior of the cornea at 10X magnification, obtaining at least 6 pictures per section with a fluorescence microscope (Zeiss Axio Observer Z1, Carl Zeiss Microimaging GmbH, Jena, Germany). The microscope settings were kept constant for all the samples. The number of remaining nuclei and nuclear debris was determined per picture using the analyze particle function of ImageJ (Maryland, USA), after applying a specific threshold (20, 255) and establishing specific size particle ranges (1.00-6.99 pixels^2 for nuclear debris and 7.00-1000.00 pixels^2 for nuclei).

The presence of alpha Gal (α-gal) epitopes and N-glycolylneuraminic acid (NeuGc), including collagen type I, in NPC and DPC was evaluated by Western Blot (WB). NeuGc and α-gal epitopes are the two main antigens that initiate the immune reaction in humans and play a critical role in the survival of xenotransplantation (Cooper *et al.*, 1993; Lee *et al.*, 2007)(Irie *et al.*, 1998; Zhu and Hurst, 2002). Corneas from each group were homogenized in Triton X-100 lysis buffer (0.5% Triton X-100, 50 mM-Tris base -pH 8.0-, 150 mM NaCl, 1 mM PMSF and protease inhibitor cocktail tablet) (Roche Diagnostics GmbH, Mannheim, Germany) using a three round of sonication for 10 second each and followed by five rounds of freeze and thaw. WB membranes were immune-stained with α-gal mouse monoclonal antibody (clone M86, ALX-801-090-1, Enzo Life Science, dilution 1:5), anti-Neu5Gc chicken polyclonal antibody (clone Poly21469, 146903, BioLegend Inc., dilution 1:1000) and anti-collagen I monoclonal mouse antibody (clone COL-1, ab90395, Abcam, dilution 1:500) followed by appropriate horseradish peroxidase secondary antibody (Abcam, Cambridge, UK). Band intensities were quantified by densitometry (ImageJ software; National Institutes of Health, Bethesda, MD).

2.3. Gamma sterilization of decellularized porcine corneas (DPC)

Gamma irradiation was performed to sterilize DPC, using a cobalt-60 source (MDS Nordion Gammacell 220E irradiator, at MIT's Department of Biological Engineering; Cambridge, MA). The samples were individually packaged in sealed glass vial filled with glycerol. The vials were placed centrally in the irradiator chamber for gamma irradiation at room temperature. The dose was calculated according to cobalt-60 source decay calculation. International Atomic Energy Agency (IAEA) recommends to use 25 kGy as the standard dose when the natural contamination level and microorganism types of the products cannot be calculated because this dose provides a maximum sterility assurance level of 10^{-6} (1990). In accordance with that, we used 25 kGy for the sterilization of DPC.

2.4. Transmission electron microscopy

Transmission electron microscopy (TEM) was performed on native human corneas (NHC), NPC, DPC and gamma irradiated DPC (G-DPC) samples. All corneal samples were fixed with half strength Karnovsky's fixative (pH 7.4) (Electron Microscopy Sciences, Hatfield, Pennsylvania) at room temperature for 30 min, then samples were placed in fresh Karnovsky's fixative for 4 hours. Then the samples were washed with 0.1 M Cacodylate Buffer (Electron

Microscopy Sciences, Hatfield, Pennsylvania) for 5min at room temperature and repeated three times. After being washed with PBS, specimens were post-fixed using 2% osmium tetroxide (Electron Microscopy Sciences) for 1.5 hours at room temperature. Then the specimens were *en bloc* stained with 2% aqueous uranyl acetate for 30 minutes, then dehydrated with ethanol, and embedded in epoxy resin (Tousimis, Rockville, Maryland, USA). Ultrathin sections (80 nm) were cut from each sample block using a Leica EM UC7 ultramicrotome (Leica Microsystems, Buffalo Grove, IL, USA) and a diamond knife, and mounted on grids. The thin sections on grids were stained with aqueous 2.5% aqueous gadolinium (III) acetate hydrate and Sato's lead citrate stains using a modified Hiraoka grid staining system (Seifert, 2017). Sections were observed by TEM with accelerating voltage at 80 kV (FEI Tecnai G2 Spirit transmission electron microscope, FEI, Hillsboro, Oregon, USA).

2.5. Optical evaluation

The optical properties of the native and treated corneas were assessed by a UV-Vis spectrometer (Molecular Devices SpectraMax 384 Plus Microplate Reader, CA, USA). Briefly, 6 mm diameter pieces were trephined from NPC, DPC and G-DPC. Subsequently, the cornea pieces were placed in a 96-well quartz microplate filled with glycerol, and the spectral transmittance of each sample was measured using the UV-Vis spectrometer. The transmittance data were recorded at 1 nm wavelength increments, from 250-850 nm. Experiments were quintuplicated and transmittance of the samples was corrected with glycerol as a blank media in quartz microplate and the mean percentage of transmittance for each group calculated and plotted as a function of wavelength.

2.6. Polarization-sensitive optical coherence tomography

A custom-built bench-top polarization-sensitive optical coherence tomography (PS-OCT) system was used to examine the depth-resolved optical polarization properties of the corneas, following the procedure previously described (Lo *et al.*, 2016; Villiger *et al.*, 2017), in order to complement the TEM approach in Section 2.4 and evaluate the collagen fibril organization in the different corneal samples mesoscopically over a large field of view. The cornea shows optical birefringence because of its characteristic orientated lamellar structure (Gotzinger *et al.*, 2004). OCT is a non-invasive high-speed volumetric optical imaging technique, which measures the spatially resolved back-scattered light from scattering samples (Hee *et al.*, 1992). The PS-OCT system consists of a wavelength-swept laser source with a center wavelength of 1320 nm and a bandwidth of 100 nm, which provides an axial resolution of 9.4 μm. The lateral resolution obtained with a 10x scan lens (Thorlabs LSM02) is ~ 10 μm. Each B-scan (cross-sectional) image is formed by 1024 A-lines. The imaging volume is 8 mm (width) x 8 mm (length) x 6 mm (depth). Corneas were rehydrated in PBS for 10 minutes before imaging. The optical birefringence, which is the difference in the refractive indices of light polarized in two different directions, can be measured by irradiating the samples using incident light of linear and circular polarizations and detecting the backscattered light using a polarization-diverse detection module (Villiger *et al.*, 2013). The intensity image was obtained via standard Fourier-transform demodulation procedures. The depth-resolved birefringence map was further reconstructed by evaluating the Stokes' vectors and employing a spectral-binning technique (Villiger *et al.*, 2013). To enhance the contrast of the map, we only report the birefringence values in areas with a sufficiently high degree of polarization.

2.7. Mechanical evaluation

The ultimate tensile strength, elongation at break and elastic modulus of the corneal tissue were measured using a Mark-10 ESM 303 (Mark-10 Corporation, NY, USA) equipped with MESUR Gauge Plus software. The instrument was equipped with a load cell of 50 N, crosshead speed was 0.5 mm/min and the initial grip separation was 6 mm. Corneal tissues (NPC, DPC and G-DPC) were dissected into dumbbell-shaped samples of the total length of 12 mm, a gage section of 4x4 mm and griping width of 6 mm. Serrated steel jaw of self-tightening grips avoided any slippage of the sample in the jaws. Samples were stress-freed prior to testing and every reported value is the average of at least four measurements using four independent corneas. The tissue sections were kept in PBS at room temperature immediately prior to the measurement. Compression Modulus was also assessed. 6 mm diameter discs from those three groups were subjected to compressive-strength measurements using a Mark-10 ESM 303 (Mark-10 Corporation, NY, USA) at a constant speed of 0.5 mm/min. During the testing, the tissue discs were preserved in PBS at room temperature immediately prior to the measurement.

2.8. Water content measurement

The water content measurement was performed on DPC, using NPC as control. Before starting the experiment, all the corneas were soaked in glycerol for two days to keep constant the conditions between the control and the DPC. After that, all the corneas were rehydrated with PBS for 2 hours. Afterwards, the wet weights of the corneas were measured after blotting with a filter paper to remove the surface water. Dry weights of all the corneas were taken after 24 hours of lyophilization. The hydrated mass ($m_{hydrated}$) and the dry mass (m_{dry}) were used to determine the water content by using the following equation.

Water content = $\{(m_{hydrated} - m_{dry})/m_{hydrated}\} \times 100$

2.9. Contact angle measurement

The surface hydrophilicity of different corneal samples - NPC, NPC where the epithelium was removed by scraping with a surgical blade (D-NPC), DPC and G-DPC - were studied by contact angle measurement. It has been suggested that angles ranging from 40 to 60 degrees might be correlated with the promotion of cell adhesion (Nara *et al.*, 2015). For that purpose, the corneas were punched with a 5mm trephine and then washed into PBS for 15 min by wild shaking the samples into the solution. Afterwards, the surface of the corneas was placed in between Whatman Quantitative Filter Papers, Ashless Grades (ash 0.007%), Grade 42 and pressed under a glass slide to remove the excess PBS and flatten the cornea. The flattening process consisted of putting a 2.5 kg weight on top of the sample for 30 min. The samples were then put onto the contact angle equipment (ramé-hart Model 590 Automated Goniometer/Tensiometer (p/n 590-U1) Ledgewood, NJ, USA). A 2 µl drop of dH_2O was deposited onto the corneas by a micro-syringe and the contact angle was measured. Each measurement was performed in less than 1 second in order to avoid any significant impact of evaporation on the measurements. Ten pictures were taken within 1 second and the average contact angle of the 10 images was computed by the DROPimage Advanced software (Ramé-hart instrument co. Succasunna, NJ, USA)

2.10. Glucose diffusivity measurements

Static Franz cell system composed of 1 ml upper cell cap and a 5 ml lower receptor chamber with the diameter of 9 mm (PermeGear 6G-01-00-09-05, PA, USA) made from borosilicate glass was used to assess the permeability of the corneal samples. 15-mm diameter discs from fresh and treated porcine corneas (NPC, DPC and G-DPC) were prepared and immediately inserted

between the two compartments, creating a barrier between the two chambers. The upper compartment was filled with 1 ml PBS and the bottom chamber was filled with a glucose solution (5 ml PBS with a glucose content of 2000 mg/dl). Both chambers were equipped with a small stirrer bar, and the solutions were mixed with a magnetic stirrer throughout the experiment, while the entire unit was placed inside of an incubator at 37°C. After glucose diffused through the corneal tissues for different time points, the glucose concentration in the upper chamber was assessed using a Counter Next EZ blood glucometer (Bayer, Parsippany, NJ, USA) with test strips. The diffusion coefficients were calculated for each tissue samples using the method previously described by Myung *et al* (Myung *et al.*, 2006).

2.11. *In vitro* biodegradation study

The resistance of DPC and G-DPC against enzymatic degradation was evaluated by collagenase from *Clostridium histolyticum* (Sigma-Aldrich, St. Louis, USA), following a previously described protocol (Islam *et al.*, 2016). NPC was tested as a control. In brief, corneas were placed in a vial containing 5U/ml collagenase in 0.1M Tris-HCl (pH 7.4) buffer supplemented with 5mM $CaCl_2$ and the experiment was carried out at 37°C. The collagenase solution was changed at every 8 hours and the percent residual mass of the sample was measured at different time points by using the following equation:

Residual mass % = W_t / W_o %

Here W_t is the weight of the sample at a certain time point and W_o is the initial weight of the sample.

2.12. *In-vitro* human plasma incubation for detection of complement activation

To prepare plasma, whole blood was collected from six healthy donors in 4.5 ml sterile tubes containing the anticoagulant lepirudin (Refludan®; Pharmion ApS, Copenhagen, Denmark) at a final concentration of 50 μg/ml (Mollnes *et al.*, 2002). The collected blood was centrifuged immediately at 3000 x g for 15 min at 4°C and 100 μl of fresh plasma from the respective donor was incubated with different cornea pieces (6 mm diameter size), namely, NPC, DPC and G-DPC. Incubations were carried out in 1.8 ml round-bottom sterile polypropylene NUNC cryotubes (Nunc, Roskilde, Denmark) for 30 minutes at 37°C. A parallel incubation with 100 μl plasma was kept for thirty minutes (T30) under the same condition to evaluate the background activation. After incubation, the reaction was stopped by adding EDTA (20 mM final concentration) and to stop further complement activation stored at -80°C until analyzed for complement activation products. The complement activation products of C4 (C4bc), C3 (C3bc) and the terminal C5-9 pathway (sC5b-9) were analyzed according to the previously described protocol (Bergseth *et al.*, 2013). Briefly, the assays were based on capture monoclonal antibodies detecting neo-epitopes exposed in the activation products after activation, hence, specifically measuring only the activation products and not the native components.

2.13. *In vitro* recellularization

2.13.1. Human corneal epithelial cells (HCEC)

Recellularization potential of DPC and G-DPC was tested using HCEC, kindly provided by Professor May Griffith; those were previously used in published work (Mirazul Islam *et al.*, 2015). HCEC grew showing a cobblestone-like appearance similar to normal corneal epithelial cells in culture. TEM showed that this cell line expresses characteristics of epithelial cells,

including desmosome formation and development of microvilli. HCEC expressed cornea epithelial cell specific 64-kD cytokeratin. Moreover, this cell line can stratify when cultured at the air-liquid interface on collagen substrates (Araki-Sasaki *et al.*, 1995).

6-mm diameter DPC and G-DPC were cut and immersed in keratinocyte serum free-medium (KSFM) at 37°C for seven days. 50,000 HCEC were seeded on top of each DPC and cultured with KSFM supplemented with 50 µg/ml bovine pituitary extract and 5 ng/ml epidermal growth factor (EGF) (Gibco, California, USA) in a 37°C and 5% CO_2 incubator. At confluence, live/dead staining was performed with a staining kit (Life Technologies Corporation, Oregon, USA), where cells were double-stained by calceinacetoxymethyl (Calcein AM) and ethidium homodimer-1 (EthD-1). On live culture, to promote stratification after confluence, the media was changed to DMEM/Ham's F-12 media (Corning, VA, USA) supplemented with 10% newborn calf serum, and 10 ng/ml EGF; and cultured for 7 days, as reported previously (Gonzalez-Andrades *et al.*, 2016). At confluence, phase contrast images were taken with 10x objectives using an inverted microscope (Nikon Eclipse TS100, Nikon Instruments Inc.; Melville, NY). After stratification, the DPC were processed for H&E staining as described above and imaged with a bright field microscope (EVOS FL Auto Cell Imaging System, Invitrogen, CA, USA).

2.13.2. Human corneal fibroblasts (HCF)

Primary human corneal fibroblasts (HCF) were also used for evaluating the recellularization potential. Cells were isolated from donated human corneoscleral rims discarded after penetrating keratoplasties performed at the Massachusetts Eye and Ear Infirmary, Massachusetts, USA. Corneal tissue was processed as previously described (Gonzalez-Andrades *et al.*, 2018), to generate corneal fibroblasts. HCF were utilized between passages 4 and 7. Like HCEC culture, HCF were also seeded on DPC and G-DPC after soaking them in DMEM/Ham's F-12 media (Corning, Manassas, VA, USA) supplemented with 10% fetal bovine serum (FBS) for seven days. 10,000 HCF were seeded on top of 6-mm diameter DPC and cultured using supplemented DMEM in a 37°C, 5% CO_2 incubator under standard culture condition for 1 month. At different time points, cell viability was measured by live/dead staining. Images were taken by using a fluorescence microscope (Zeiss Axio Observer Z1, Carl Zeiss Microimaging GmbH, Jena, Germany).

2.13.3. Human corneal endothelial cells (CEC)

CEC, kindly provided by Professor Ula Jurkunas, were cultured on the top of the DPC and G-GPC, after soaking the tissues in Opti-MEM I with Glutamax-I media (Life Technologies Corporation, Carlsbad, CA) supplemented with 8% (v/v) FBS (Life Technologies Corporation), 5 ng/ml EGF (EMD Millipore Corporation, Temecula, CA), 0.2 mg/ml calcium chloride (Fisher Scientific Company, Fair Lawn, NJ), 0.8 mg/ml chondroitin sulfate-A (Sigma-Aldrich, St. Louis, MO), 0.25 mg/ml Gentamycin (Life Technologies Corporation), 1% (v/v) Antibiotic-Antimycotic solution (Life Technologies Corporation), 0.1 mg/ml bovine pituitary extract (Alfa Aesar, Ward Hill, MA) for seven days. 20,000 CEC were seeded on the xenograft with the same media that was used for soaking the grafts. Live/dead staining was performed after seven days of culture. Media was changed every other day.

2.13.4. Hybrid neuroblastoma cells (NDC)

NDC were also kindly provided by May Griffith, whose lab extensively used NDC as a source of neural progeny to evaluate biocompatibility on different biomaterials (Hackett *et al.*, 2010; Koh *et al.*, 2013). For culturing NDC, xenografts were soaked in DMEM media (Sigma-Aldrich)

supplemented with 10% (v/v) FBS (Life Technologies Corporation) for seven days. 20,000 NDC were cultured directly on the top of DPC and G-DPC to evaluate the potential of the decellularized xenograft to support neural growth. At day seven, live/dead staining was performed to evaluate the cells viability of the xenografts.

2.14. Immunohistochemistry (IHC)

The expression of cytokeratin 3+12 and mucin MUC16 by HCEC after recellularization on DPC and G-DPC was determined by fluorescence immunohistochemistry, using paraffin embedded tissue sections. The same paraffin embedding protocol was used as described above. For IHC, paraffin was removed from the tissue sections, using xylene, and the samples were rehydrated in water through a graded series of alcohols (100%, 96%, 70%, 50%, and water). For antigen retrieval, tissue sections were incubated with 10mM Sodium citrate buffer, 0.05% Tween 20 (pH 6.0) at 60°C for overnight. The sections were washed with Tris-buffered saline (TBS) plus 0.025% Triton X-100 followed by blocking any unspecific binding sites using TBS supplemented with 10% FBS and 1% bovine serum albumin (BSA). The sections were then incubated with the primary antibodies overnight at 4°C in humidifying condition. Mouse monoclonal antibody against corneal epithelial cell specific cytokeratin (anti-cytokeratin 3+12, clone AE5; ab68260, Abcam) and mouse monoclonal antibody against corneal mucin (anti-MUC16, clone X75; ab10029, Abcam) were used separately at dilution 1:50 and 1:300, respectively. Incubation with secondary antibodies was carried out for 1 hour at room temperature. TRITC-conjugated anti-mouse antibody (ab6786, dilution 1:100; Abcam) and FITC-conjugated anti-mouse antibody (ab6785, dilution 1:100; Abcam) were used as secondary antibody for cytokeratin 3+12 and mucin, respectively. Finally, slides were mounted in VectaShield mounting medium containing DAPI (Vector Laboratories, Inc., CA, USA), and examined by an inverted fluorescent microscope (Zeiss Axio Observer Z1, Carl Zeiss Microimaging GmbH, Jena, Germany) with a 40x objective.

2.15. *Ex vivo* transplantation into pig eyes

The feasibility of the DPC and G-DPC to be used as a donor tissue for anterior lamellar keratoplasty (ALK) and as a carrier for Boston Keratoprosthesis Type 1 (BKPro) was tested in *ex vivo* condition on pig eyes. BKPro is the most commonly used worldwide artificial cornea in severe corneal diseases that have poor prognosis for standard treatment. The BKPro is a double-plated device, mainly made of polymethyl methacrylate (PMMA), which usually requires a fresh corneal graft as a carrier (Gonzalez-Andrades *et al.*, 2018).

For ALK, host pig cornea was half-thickness trephined with an 8 mm Barron trephine and approximately half of the thickness of the host tissue was removed using a crescent blade. DPC and G-DPC were then trephined at 8 mm and split to half thickness to obtain the donor graft. Subsequently, the graft was transplanted into the previously prepared 8 mm host corneal bed using eight interrupted 10-0 nylon sutures.

A different experimental procedure was followed for the implantation of BKPro. Eleven mm diameter discs of DPC and G-DPC were centrally trephined with a 3 mm trephine. The standard procedure of assembly of BKPro (type 1,) and donor tissue was followed (Todani *et al.*, 2011). Eleven mm diameter full thickness trephination of the host cornea was performed. Afterwards, BKPro-graft combination was placed in the host bed and sutured with eight interrupted 10-0 nylon sutures.

A digital microscope (Dino-Lite Edge 3.0, New Taipei City, Taiwan) was used to capture the image of the transplanted eyes. OCT images were obtained using a Heidelberg Spectralis HRA + OCT (Heidelberg Engineering GmbH, Heidelberg, Germany).

2.16. Statistical Analysis

Comparisons between multiple groups were analyzed by ANOVA with Dunnett's post hoc analysis as all groups were compared with the control group (NPC). Data were log transformed before analysis to comply with the assumptions of general linear models. One-way ANOVA with Tukey post hoc was done among the groups to compare mechanical and functional characteristic properties. Significance difference for WB was determined using ratio paired Tukey's post hoc multiple comparison tests. A value of $P < 0.05$ was considered statistically significant. n.s., *, **, ***, and **** represent $p > 0.05$, $p < 0.05$, $p < 0.01$, $p < 0.001$ and $p < 0.0001$, respectively. GraphPad Prism Software (GraphPad Software, CA, USA) was used to analyze the data.

3. RESULTS

3.1. Evaluation of decellularization process

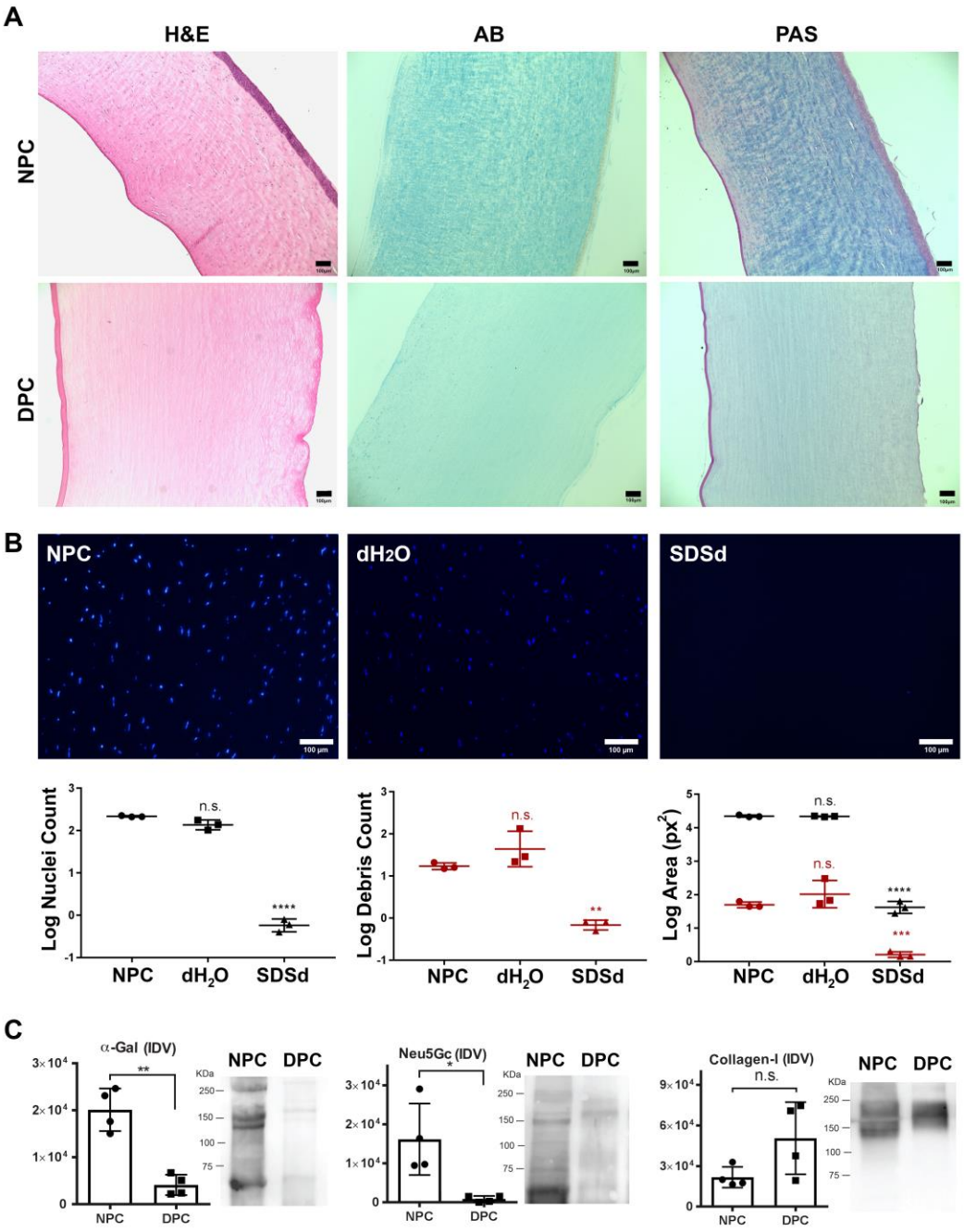

Fig. 1. Assessment of the decellularization process. (A) Histological evaluation by staining with Hematoxylin and Eosin (H&E), Alcian Blue (AB) and Periodic Acid Schiff (PAS) on decellularized porcine cornea (DPC) compared with native porcine cornea (NPC). (B) Confirmation of decellularization by DAPI staining of nuclei and nuclear debris within NPC, corneas treated with distilled water (dH_2O) and corneas treated with SDS in distilled water (SDSd). Graphs represent the nuclei (black color) and nuclear debris (red color) count and area covered by them. The results were reported as the mean ± S.D. and significance compared with NPC. Scale bars: 100 µm. (C) Specific detection of α-gal, Neu5Gc and collagen-I by Western Blot (WB) in NPC and DPC. The integrated density value (IDV) of each band was measured. Bar charts represent the calculated intensity of corresponding proteins using ImageJ

densitometry. The results were reported as the mean ± S.D. from four independent corneas. Representative images of the WB are shown on the right.

Histological evaluation of NPC and DPC was performed (Fig. 1A). H&E staining showed that corneal epithelial cells, stromal cells, and endothelial cells were distinctly visible in the NPC. However, in the DPC, no epithelial, stromal or endothelial cell could be observed. H&E also confirmed that decellularized cornea had a slightly increased thickness compared to NPC. AB staining on NPC showed the presence of GAG throughout the cornea with a higher concentration at the anterior part. Conversely, DPC showed an intense reduction of GAG that extended to the entire corneal stroma. PAS-stained carbohydrates were mainly present in the anterior two thirds of the stroma in NPC. In contrast, carbohydrates concentration by PAS was highly reduced in DPC. PAS staining of DPC showed the presence of an intact epithelial basement membrane and Descemet membrane.

DAPI staining revealed that 0.1% SDS solution in distilled water (SDSd) was able to significantly remove cells from all cellular layers of the porcine cornea compared to the native cornea and cornea treated with dH_2O (Fig. 1B). In order to evaluate the effectiveness of the decellularization, we measured the residual number of nuclei and nuclear debris that remained on DPC after decellularization. DAPI staining indicated that the number of nuclei and area of the nuclei were significantly reduced in DPC compared to NPC ($p=0.0001$ for both comparisons). Nuclear debris count and area measurement also follows the nucleus measurement, showing that DPC was significantly free from debris compared to NPC ($p=0.0010$ and $p=0.0006$, respectively).

WB analysis confirmed that after decellularization, the presence of α-gal and NeuGc in the cornea was significantly reduced compared to the native cornea, $p=0.0089$ and 0.0454, respectively (Fig. 1C). Non-significant differences in collagen type I content was observed following decellularization ($p=0.1619$).

3.2. Transmission electron microscopy (TEM)

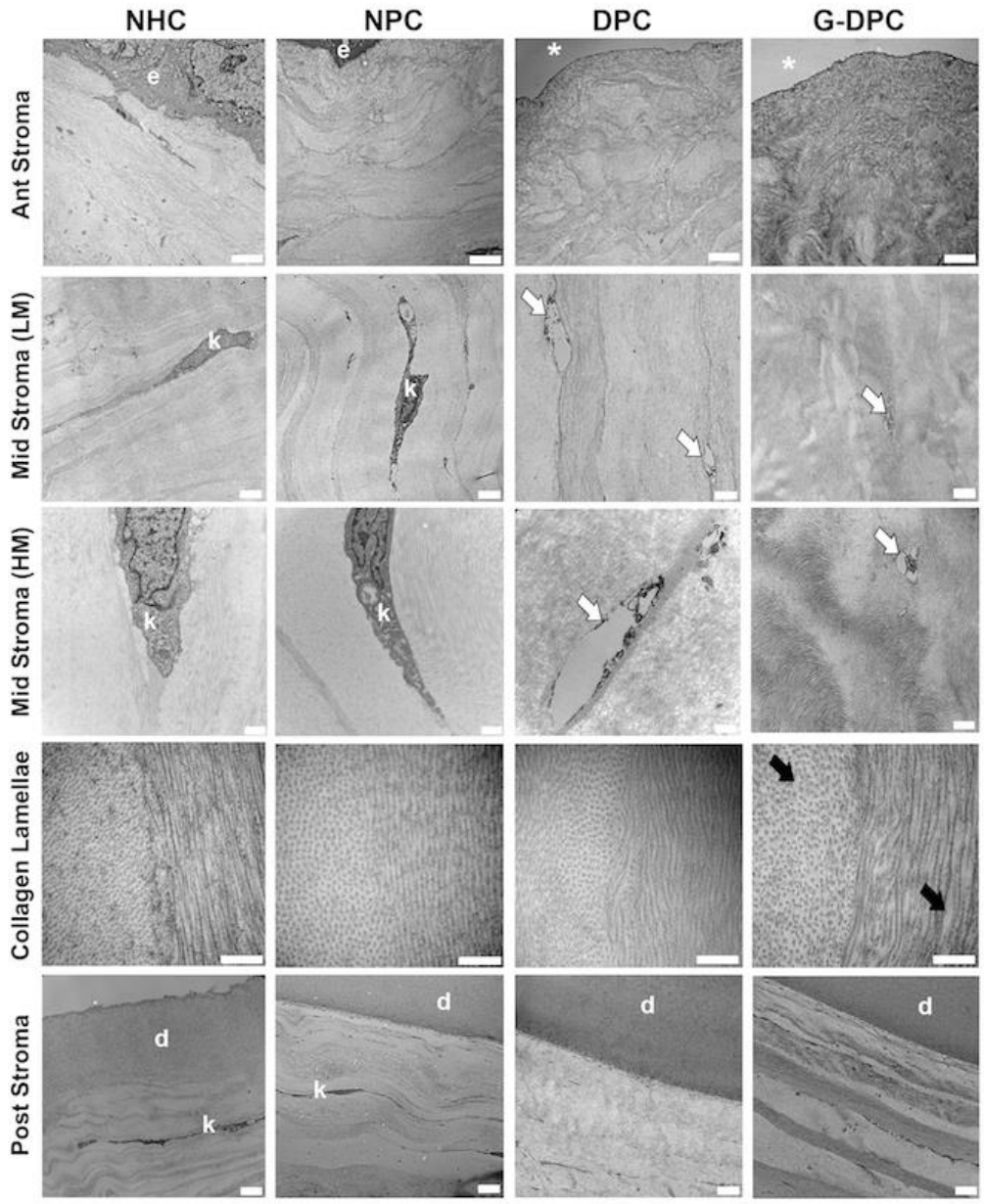

*Fig. 2. Transmission electron microscopy (TEM) micrographs of native porcine corneas (NPC), decellularized porcine cornea (DPC) and gamma irradiated decellularized porcine cornea (G-DPC); compared with native human cornea (NHC) at different layers of the cornea and at different magnification (LM, low magnifications and HM, high magnification). e: epithelium; *: absence of epithelium; k: keratocyte; white arrows: presence of debris after decellularization; black arrows: increased space between collagen fibrils after gamma irradiation; d: Descemet membrane. Scale bars: for 1st, 2nd and 5th row, 2 µm; for 3rd row, 500 nm; for 4th row, 100 nm.*

The structural organization of the stroma of non-gamma and gamma irradiated decellularized corneas, including the presence of cell debris, was compared with NPC and NHC through TEM (Fig. 2). In these two cellular groups of corneas, keratocytes were visualized with low (LM) and high magnification (HM) images in the stroma. LM and HM images of mid-stroma of DPC and G-DPC confirmed the removal of the cells, leaving vacant spaces in the stroma. HM images of DPC and G-DPC revealed the presence of some cell debris. The ultrastructure of the

extracellular matrix of the stroma and the Descemet membrane of decellularized corneas were similar to native corneas. Highly ordered and stacked collagen lamellae were observed in all the groups. In DPC and G-DPC, the collagen lamellae within the stroma were arranged parallel to each other, similar to NHC and NPC. The collagen fibrils within the lamellae showed a similar diameter in all the groups. However, the inter-fibril space varied among the different groups, observing an increase of heterogeneity in the decellularized groups, being higher in G-DPC compared to DPC.

3.3. Optical evaluation

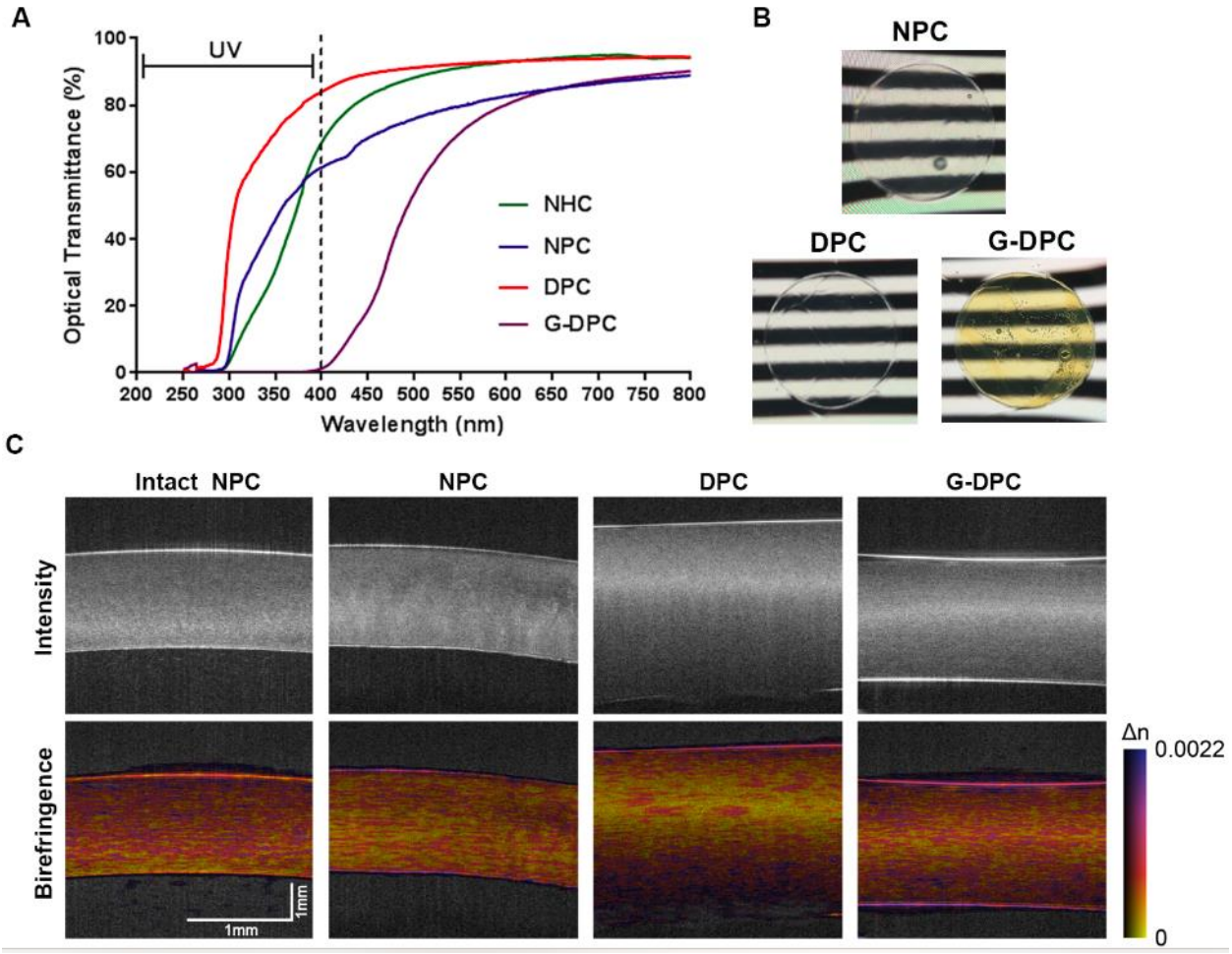

Fig. 3. Optical evaluation of decellularized and sterilized porcine corneas. (A) Light transmission through the native human cornea (NHC), native porcine cornea (NPC), decellularized porcine cornea (DPC) and gamma irradiated decellularized porcine cornea (G-DPC); from UV to visual wavelengths. (B) Macro pictures of porcine corneas after different treatments placed on a black-white stripe pattern projected on a self-illuminated screen. (C) Intensity (conventional OCT) and birefringence (PS-OCT) images of the intact porcine cornea before extraction from the eye globe (intact NPC), together with native and treated corneas. The color bar of the birefringence images displays a range of refractive index contrast from 0 to 0.0022. The birefringence values were only plotted in areas with sufficiently high degree of polarization.

The UV-Vis spectroscopy revealed that the final product after decellularization was transparent (Fig. 3A). However, transparency varied during the different steps of the decellularization process. DPC became transparent similar to native porcine and human corneas at the visual wavelength (400 to 700 nm). Moreover, DPC transmitted approximately 60% of the UVB light. On the other hand, G-DPC showed 40% absorption of light at the blue band with wavelengths ranging from 400 to 499nm, and gamma irradiation caused the yellow appearance of the G-DPC (Fig. 3B). Moreover, G-DPC showed complete blocking of UV light from 250 to 400 nm. At the far visual wavelengths (around 600nm), G-DPC were transparent to visual light, similar to NPC.

Intensity images of OCT confirmed the thickness and integrity of the corneal stroma. Intact NPC and NPC after rehydration showed the same thickness (Fig. 3C). The thickness of the stroma increased after decellularization and again reduced close to NPC after gamma treatment in G-DPC. Certain depths of the corneas appear to be more strongly scattering due to the focusing effect of the curved cornea samples. Birefringence images of the PS-OCT, which showed additional contrast beyond the conventional intensity OCT, revealed that in NPC the differences of the refractive indices were high and were equally distributed throughout the stroma. The degree of birefringence was less prominent and more spread out in the swollen DPC compared to the NPC. After gamma irradiation, the thickness was reduced, and birefringence was high throughout the cornea, which was similar to NPC.

3.4. Mechanical characterization of different porcine and human corneas

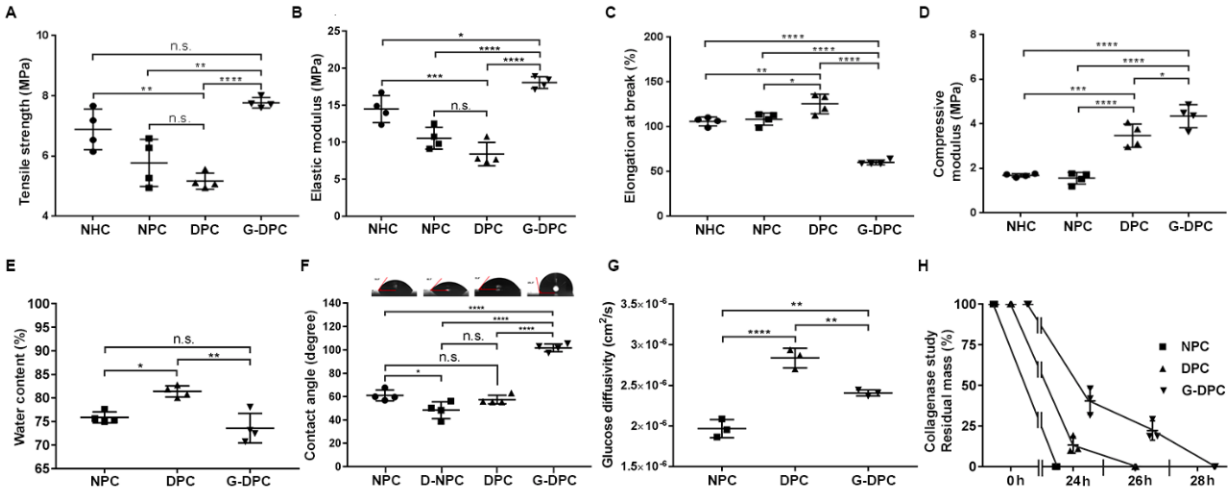

Fig. 4. Mechanical and functional assessment of decellularized and sterilized porcine corneas. (A-D) Mechanical properties comparison among native human cornea (NHC), native porcine cornea (NPC), decellularized porcine cornea (DPC) and gamma irradiated decellularized porcine cornea (G-DPC). (E-H) Functional characteristic comparison among different cornea samples. (F) Micrographs of water contact angle of different corneas were placed on the top of the respected groups at contact angle measurement graph; D-NPC: deepithelialized NPC. (H) For collagenase study, the residual masses were presented against time in hour. For all panels, quantitative results were reported as the mean ± S.D. from four independent experiments and results were compared between the groups for statistical analysis.

GI positively changed the mechanical properties of the decellularized xenograft, becoming stiffer than non-irradiated DPC (Fig. 4A-D). Tensile strength of G-DPC was similar to NHC ($p=0.1495$) but significantly higher compared to DPC ($p<0.0001$) and NPC ($p=0.0011$) (Fig. 4A). Although,

there was not significant difference in elastic modulus between NPC and DPC, G-DPC demonstrated higher elastic modulus surpassing that of NHC and NPC (Fig 4B). Moreover, while DPC had higher elongation at break than NHC and NPC, G-DPC showed decreased value compared to NHC, NPC and DPC (Fig 4C). We also measured the compressive modulus of different corneas until 40N load, as the corneas were not breakable by the machine we used (Fig. 4D). Similarly, G-DPC showed lower compressibility compared to the other groups as indicated by higher compressive modules.

3.5. Functional characteristic comparison among different porcine corneas

Water content of DPC was 81.3 ± 1.0%, which was significantly higher than that of G-DPC (73.6 ± 2.7%) (Fig 4E) and similar to human corneas (78.0 ± 3.0%) (Rafat *et al.*, 2008). G-DPC had the lowest water content although non-significantly different from human corneas. Water contents were similar for NPC and G-DPC whereas, NPC versus DPC and DPC versus G-DPC differ significantly, p= 0.0108 and p=0.0012, respectively.

Contact angle, demonstrating the wettability of a solid surface, was investigated (Fig. 4F). Water placed on intact corneal epithelium showed significantly greater contact angles (mean, 60°) than water placed directly on Bowman's layer on deepithelialized NPC (D-NPC) (mean, 48°; p=0.0165). DPC has contact angle measurements similar to NPC and D-NPC. The wettability of G-DPC (mean, 101°) was significantly decreased from DPC (p<0.0001), NPC (p <0.0001), and D-NPC (p <0.0001).

Glucose diffusivity of DPC was significantly higher than NPC (p <0.0001) and G-DPC (p= 0.0039) (Fig. 4G). Glucose diffusivity of G-DPC was also significantly higher than NPC (p= 0.0036).

Biodegradation was assayed *in vitro* by collagenase degradation assay measuring the relative resilience of DPC compared to G-DPC (Fig. 4H). G-DPC took two hours more to be completely digested compared to DPC and 4 hours more compared to NPC (28, 26 and 24 hours, respectively). After 12 hours of collagenase exposure, only 25% of the residual mass was preserved for DPC, whereas, more than 50% of the residual mass was preserved for G-DPC.

3.6. Complement activation in contact with human plasma

The three activation products C3bc (Fig. 5A), C4bc (Fig. 5B), and sC5b-9 (Fig. 5C) were assessed to examine the potential effects of the differently treated porcine corneas on human complement activation using six donors. Although the C4bc values were higher in NPC than the treated corneas (DPC and G-DPC) and sC5b-9 values were higher in the G-DPC group, there were no significant differences between any of the groups.

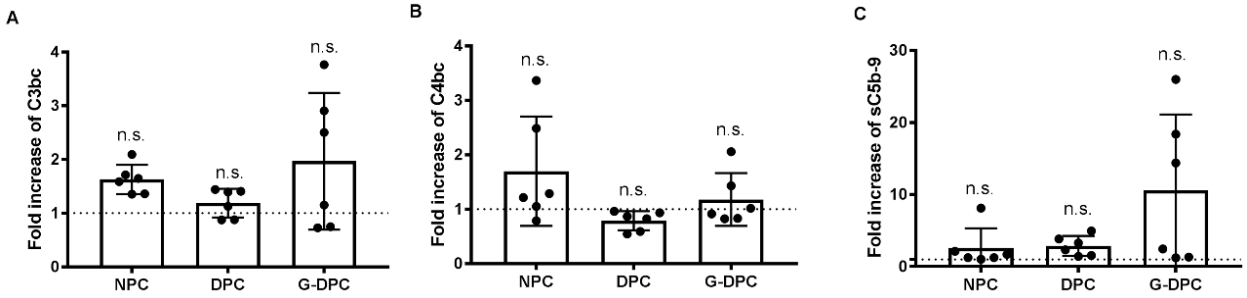

Fig. 5. Complement activation induced by native porcine cornea (NPC), decellularized porcine cornea (DPC) and gamma irradiated decellularized porcine cornea (G-DPC) after incubation in normal human plasma for 30 minutes at 37℃. (A) C3-activation (C3bc), (B) C4-activation (C4bc) and (C) terminal pathway activation (sC5b-9) are reported as fold increase related to the background activation in plasma without any corneas (indicated with a dotted line). The bars show mean fold increase ± S.D. of six independent experiments.

3.7. Recellularization of DPC and G-DPC

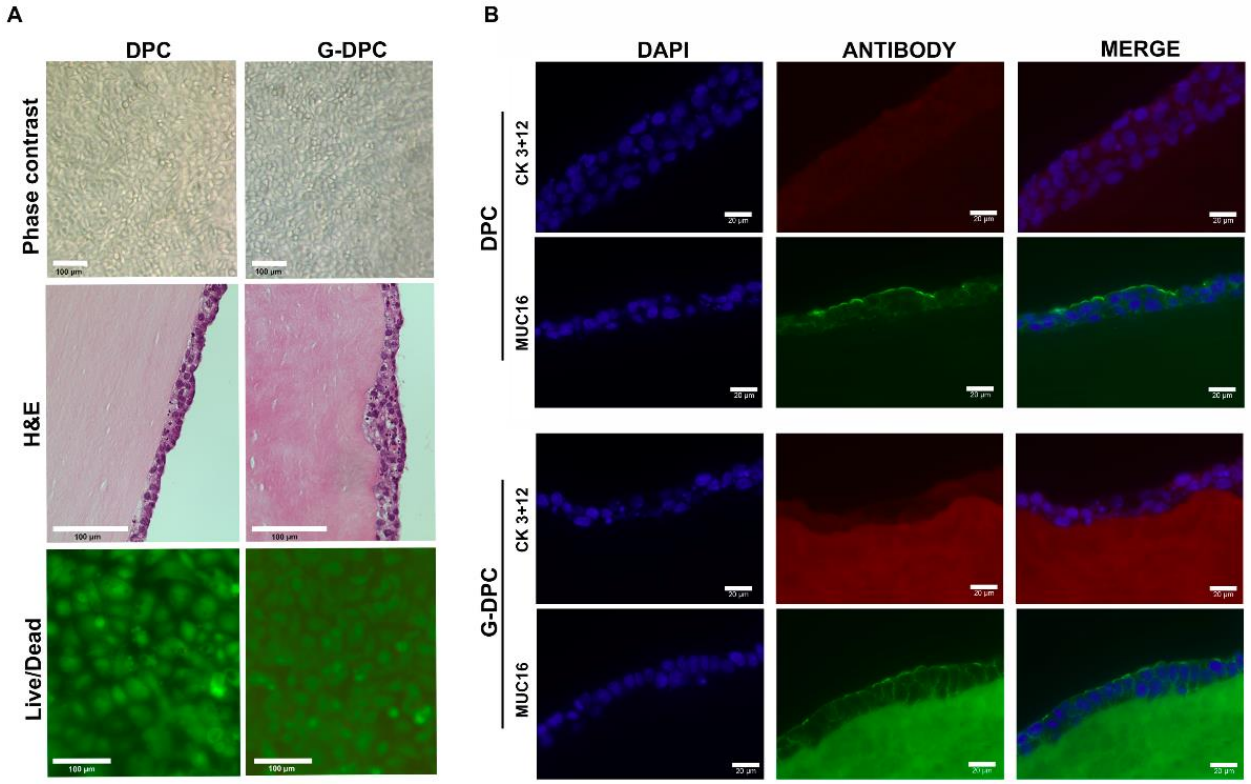

Fig. 6. Evaluation of the recellularization process. (A) Corneal epithelial recellularization on decellularized porcine cornea (DPC) and gamma irradiated decellularized porcine cornea (G-DPC), showing cell monolayers by phase contrast microscopy and stratified epithelia by Hematoxylin and Eosin (H&E) on the anterior surface of DPC and G-DPC. Live/dead showed the cytotoxicity, where green cells are live cells and red cells are dead cells. Scale bars: 100 µm. (B) Representative fluorescence microscope images of the expression of cytokeratin 3+12 (CK 3+12) (red) and mucin (MUC16) (green) by human corneal epithelial cells on DPC and G-DPC. Nuclei were stained with DAPI (blue). Scale bars: 20 µm.

To determine the recellularization efficiency of decellularized tissues, HCEC, HCF, CEC and NDC were seeded on the surface of DPC and G-DPC (Fig. 6A). Phase contrast microscopy images of DPC and G-DPC recellularized with HCEC demonstrated that epithelial cells were able to attach, migrate and proliferate on both surfaces when cultured with supplemented KSFM media. At confluence, upon changing media to stratification media, cells formed stratified layers of 3-4 cells on both types of decellularized tissue, which was confirmed by H&E staining. Phenotypic evaluation of HCEC grown on DPC and G-DPC was carried out by

immunohistochemistry (Fig. 6B). HCEC cultured on DPC and G-DPC expressed cytokeratin 3+12 and MUC16. Autofluorescence from decellularized tissue, especially G-DPC, compromised the picture quality.

HCF were cultured on the surface of DPC and G-DPC for one month and live/dead staining was performed at 15 days and one-month time points to check the cytotoxicity of the tissues (Fig. 7). There were very few dead cells (red) remaining. Both surfaces became confluent with HCF (green) in a similar fashion. A similar result was observed for CEC, which created a monolayer of viable cells on DPC and G-DPC, as visualized with live/dead staining. Negligible numbers of dead cells on both types of xenograft were observed. NDC, a neural progenitor cell, also grew on the DPC and G-DPC, showing that both types of decellularized tissues have the potential to support neural cell growth.

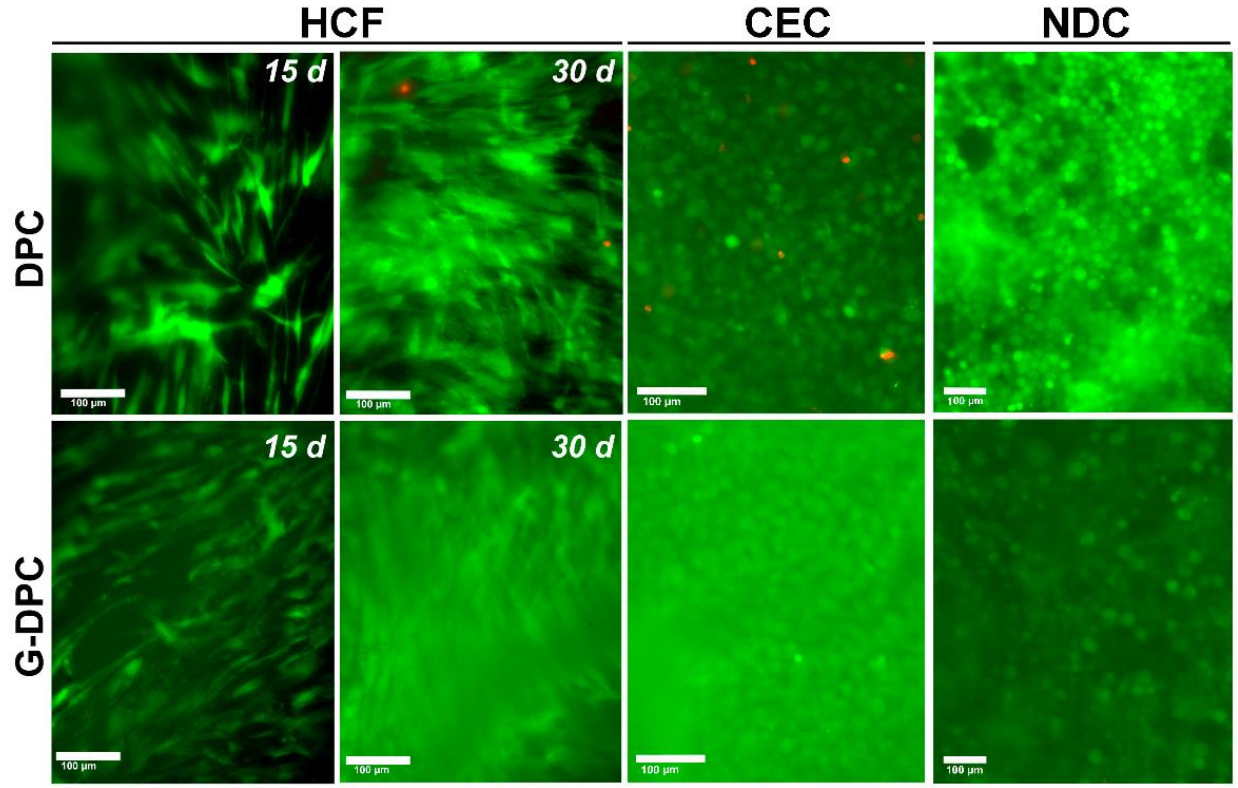

Fig. 7. Live/dead staining of human corneal fibroblasts (HCF), human corneal endothelial cells (CEC) and neural progenitor cells (NDC) on decellularized porcine cornea (DPC) and gamma irradiated decellularized porcine cornea (G-DPC). Scale bars: 100 µm.

3.8. *Ex vivo* transplantation of corneas into pig eyes

Both DPC and G-DPC were transplanted into pig eyes *ex vivo* by anterior lamellar keratoplasty and used as a carrier for BKPro implantation (Fig. 8). The xenografts could be effortlessly sutured to the host tissue, showing a similar behavior to human corneas. Slit lamp biomicroscopy and OCT images showed that the implant remained stable into the host eye immediately after the surgery. OCT images confirmed the apposition of the implanted tissue with the host cornea after ALK and BKPro. OCT image of the BKPro transplanted eye confirmed the stable assembly of BKPro into the carrier xenograft.

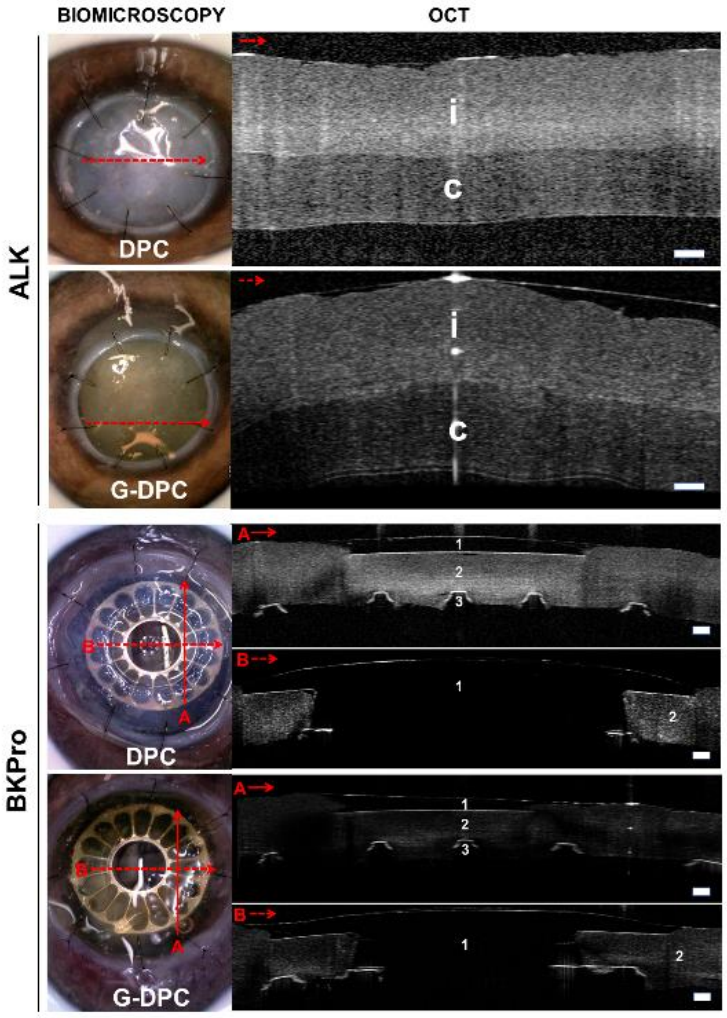

Fig. 8. Biomicroscopy and OCT images of non-gamma (DPC) and gamma irradiated (G-DPC) decellularized porcine corneas transplanted ex vivo in pig eye as anterior lamellar grafts and as a carrier for BKPro. Red arrows on the slit lamp images represent the section and direction of the OCT. No gaps within implanted donor cornea (i) or host corneas (c) were observed in either model. 1, 2 and 3 represent BKPro front plate (made of PMMA), donor cornea and BKPro black plate (made of titanium), respectively. Scale bars: 200 µm.

4. DISCUSSION

In the present study, we evaluated the effect of sterilizing decellularized porcine corneas for transplantation using GI. We show that this process is not deleterious for the tissue and allows retention of physiological, mechanical and optical properties needed for corneal transplantation. One of the main reasons to use GI as sterilization method for decellularized cornea was that it had been successfully applied to sterilize human donor corneas that are used in human patients (Daoud *et al.*, 2011), including as carriers for the BKPro (Fadlallah *et al.*, 2014), and decellularized porcine corneas used in clinical studies (Zhang *et al.*, 2015)(Shi *et al.*, 2017).

Different decellularization protocols have been used over time with mixed success (Kim and Hara, 2015). Most of the protocols are based on the anionic detergent SDS. This detergent displays a high water binding capacity based on its negative charge, which causes the swelling of the tissue, and facilitates SDS penetration and the lysis of the cells (Du *et al.*, 2011). Various concentrations of SDS were studied previously to determine an effective decellularization concentration without reducing the GAG and collagen content of decellularized corneas (DC). In many cases, SDS treatment was applied on enzyme-treated samples (Yoeruek *et al.*, 2012a, b). Some reports have demonstrated that a high concentration of SDS decreased the GAG content, damaged basement membrane and loosened the collagen fibrils (Pang *et al.*, 2010; Sasaki *et al.*, 2009). We used a 0.1% SDS solution as we have previously shown that corneas treated with this concentration contained less residual nuclear debris (Gonzalez-Andrades *et al.*, 2011). We were able to optimize the decellularization effectiveness by changing the solvent of the solution. As we have reported here, 0.1% SDS in dH_2O removed almost all the cellular content of DPC compared to the native untreated control, without significantly disrupting the corneal extracellular matrix. Our H&E and DAPI staining confirmed the removal of the cellular component from the DPC, and the swelling of the DPC, a common consequence of decellularization (Shafiq *et al.*, 2012) that could be associated to the GAG reduction observed in Alcian blue staining (Mendoza-Novelo *et al.*, 2011). PAS confirmed epithelial basement membrane integrity in DPC. We also showed that the decellularization process significantly reduces the presence of α-gal and NeuGc in the DPC, without decreasing collagen type I. α-gal (Sandrin and McKenzie, 1994) and NeuGc (Padler-Karavani and Varki, 2011) are the main pig specific xenoantigens recognized by human natural antibodies, which mainly limit the fate of the xenotransplantation. Thus, we describe a very simple and effective decellularization protocol that preserves the corneal extracellular matrix. Moreover, taking into account the inexpensiveness of the reagents used, this protocol is feasible and easily applied, and may be useful in low-income countries, where most of the corneal blind patients live.

Distortion of the ultra-structure of the collagen lamellae of the cornea is an undesirable effect of the decellularization and sterilization processes. By TEM analysis of treated and untreated corneas, no gross changes were noted in collagen fibers for DPC compared to NHC and NPC, except that the fibers were marginally larger. This might be due to swelling as previously described by other researchers (Shafiq *et al.*, 2012). The fact that gamma irradiation reduced swelling, which brings back the regular spacing and ordering between the collagen lamellae, might be correlated with the resumption of birefringence in G-DPC back to the NPC level via the PS-OCT analysis. Moreover, distortion of the collagen lamellae can cause a decrease in corneal transparency. SDS treated DPC and G-DPC became transparent after soaking in glycerol. This effect of glycerol was similar to a previous report (Pang *et al.*, 2010). Regarding the UV transmission in GI samples, we observed that G-DPC treated with glycerol were able to completely block UV transmission. However, another research group has recently reported that gamma irradiated porcine corneas were equally transparent at 280 nm to 780 nm compared to non-gamma irradiated cornea (Lin *et al.*, 2017). Thus, following our protocol, UV protection

would not be a necessary precaution for corneal transplanted patients as it was recommended, for example, to patients transplanted with collagen-based artificial corneas until the epithelium repopulated the scaffold (Fagerholm *et al.*, 2010).

We also observed that gamma irradiated samples turned pale yellow. This yellowing effect has been already described in gamma irradiated human corneas, BKPro front plates and other polymers different to PMMA, associated to chain scission of the materials (Gonzalez-Andrades *et al.*, 2018). As GI can break chemical bonds as well as crosslink polymers (Cheung *et al.*, 1990), fragmented collagen chains undergo a secondary crosslinking which ultimately contributed to favorable mechanical properties and resistance to enzymatic degradation, keeping cornea compact even without the presence of a healthy endothelium (Yoshida *et al.*, 2015)(Leontiou *et al.*, 1993; Bailey *et al.*, 1964; Tzaphlidou *et al.*, 1991). In this regard, mechanical property measurements revealed that G-DPC were the strongest showing a high tensile strength, similar to NHC. The high elastic modulus of G-DPC was in the range of other types of tissues, such as cartilage or cortical bone (Lai *et al.*, 2015), which suggest that these xenografts could be applied not only as corneal or scleral substitutes but also as tissue replacement in extraocular areas of the body. Additionally, GI also modified the contact angle of the corneal surface. However, the higher contact angle showed by G-DPC was not associated to an impairment of the recellularization process with any of the cells studied in this work.

Additionally, collagenase experiments revealed that both kinds of decellularized corneas were stable more than 24 hours, similar to native corneas and more resistant than other type of corneal substitutes made of collagen that degrade approximately after 10 hours in collagenase (Merrett *et al.*, 2009; Liu *et al.*, 2008). Furthermore, those stromal changes induced by the decellularization and irradiation processes did not impair glucose diffusion, keeping an optimal porous structure of the cornea that permits the adequate distribution of solutes and nutrients throughout its structure (Sweeney *et al.*, 1998). Glucose diffusivity of DPC and G-DPC was found $(2.80 \pm 0.04)x10^{-6}$ cm/s^2 and $(2.35 \pm 0.05)x10^{-6}$ cm/s^2, respectively, which was as good as the diffusivity already reported for human native corneas $(2.60 \pm 0.3)x10^{-6}$ cm/s^2 (McCarey and Schmidt, 1990).

Complement is activated as a recognition system both through pathogens, damaged self-structure and due to cross-species incompatibility like as described for pig and humans. Conformational changes of the extracellular matrix due to decellularization might influence immune activation, as has been observed by other research groups (Bastian *et al.*, 2008). Our experiments showed that there was no significant difference in complement activation between treated corneas compared to native corneas. It should be emphasized, however, that the number of experiments were limited and further investigation of the innate immune activation would be needed on a broader basis in the future, including activation of the cytokine network.

Recellularization of a decellularized xenograft is one of the most important steps to characterize them as functional corneal substitutes. Here, we observed that DPC and G-DPC both facilitated the growth and migration of human corneal epithelial cells, corneal fibroblasts, corneal endothelial cells and NDC despite changes observed in the corneal extracellular matrix after decellularization and GI. GI-treated tissues had no cytotoxic effect, as shown by Gorham *et al*., using mouse foreskin fibroblasts (Gorham *et al.*, 1993). Our cell study results are in the agreement with previous studies that described the capability of HCEC (Yoeruek *et al.*, 2012a) and HCF (Gonzalez-Andrades *et al.*, 2011) to grow on DPC treated with SDS. However, when human corneas were decellularized and recellularized with human corneal epithelial cells and fibroblasts, SDS treated corneas favored the growth of fibroblasts over epithelial cells (Shafiq *et al.*, 2012). This difference might be due to the different species used or differences on the

decellularization, sterilization and recellularization protocols applied to the corneas even when SDS were used in all of them.

Here, we also investigated the growth of epithelium and showed that terminally differentiated corneal epithelial cells were able to grow on top of DPC and G-DPC, expressing specific terminally differentiated epithelial corneal markers such as cytokeratin 3 and 12. Cytokeratin 3 and 12 are expressed throughout the full thickness of the human corneal epithelium (Schermer *et al.*, 1986; Kiritoshi *et al.*, 1991), which correlated with the expression pattern we found in the recellularized samples. Furthermore, epithelial cells cultured on the decellularized corneas were able to synthesize a protective mucin layer that stained with MUC16. MUC16 is a heavily glycosylated transmembrane protein expressed by the matured apical and subapical flattened cells of the human corneal epithelium. It is localized on the tips of the surface microplicae, providing an anti-adherent barrier to the epithelial layer, which is crucial for the homeostasis of the epithelium (Shirai *et al.*, 2014). It was shown before that immortalized human corneal cells express MUC16 (Gipson *et al.*, 2003), characteristically expressed in the epithelial surface microplicae (Gipson *et al.*, 2014). We found the same pattern in the stratified epithelium that we cultured on the decellularized corneas. Both types of decellularized xenografts also supported corneal endothelial cell growth. It was previously shown that SDS treated porcine cornea facilitated CEC growth in in-vitro culture condition (Ju *et al.*, 2012). To our knowledge, this is the first report making use of the NDC cell line to evaluate neural growth in xenografts. This cell line is a hybrid created by fusion of the two cell types; rodent dorsal root ganglion and neuroblastoma (Wood *et al.*, 1990). These cells have the properties of growing as mature sensory neurons and can extend neurites and produce substance P (Wood *et al.*, 1990; Newman *et al.*, 2006). NDC were able to grow on both types of decellularized xenografts, showing the potential of the graft to allow an optimal reinnervation once implanted.

The *ex vivo* work showed the feasibility of using G-DPC as corneal substitute not only for regular keratoplasties but also as a carrier for BKPro implantation. However, to show convincing evidence for the beneficial effect of G-DPC in clinical practice, we need a long-term *in vivo* study using optimal animal models. The animal model used should be representative of humans in terms of biointegration and biocompatibility. In this regard, the only model that mimics the human response to xenografts, including the presence of natural antibodies against alpha gal epitope, is Old World primates (Huai *et al.*, 2016). Choi *et al.* performed one of the very few studies where Old World primates were used to evaluate decellularized non-irradiated xenografts. Decellularized and fresh porcine corneas were compared by transplanting into rhesus macaques. This study was carried out in presence of high doses of immune suppressive agents and half of the fresh cornea developed chronic rejection whereas 80% of the DPCs remained transparent for more than 6 months (Choi *et al.*, 2011).

5. CONCLUSION

In conclusion, in the present study we evaluated the effect of sterilizing decellularized porcine corneas for transplantation using gamma irradiation. According to our results, this sterilization method is not deleterious for the tissue and allows retention of physiological, mechanical and optical properties required for corneal transplantation. Additionally, we optimized a simple and inexpensive decellularization protocol based on SDS to efficiently remove most of the antigenic elements of porcine corneas. The use of this decellularization protocol combined with gamma radiation sterilization emerges as a promising approach to treat human patients as an alternative to the corneal allograft.

6. ACKNOWLEDGEMENT

This paper was supported by Boston-KPro research fund and NIH National Eye Institute Core Grant P30EY003790. Financial support was also obtained from The Odd Fellow Foundation and The Simon Fougner Hartmann Family Fund. PCH was supported by the Croucher Fellowship. MG and JK acknowledge the support of HK ITC grant reference: ITS/195/14FP. Access to the PS-OCT instrumentation and processing tools was provided by the Center for Biomedical OCT Research and Translation, which is supported by the Nationals Institutes of Health (grant P41EB-015903).The authors gratefully acknowledge support from the Department of Biological Engineering of MIT for gamma irradiation and. Oscar Morales (Schepens Eye Research Institute) for assisting with the OCT *ex vivo* work. We also appreciate the aid of Bianai Fan and Philip Seifert (Schepens Eye Research Institute) in the light and electron microscopy studies, respectively.

7. DISCLOSURES

Mohammad Mirazul Islam, Roholah Sharifi, Dina B. Abusamra, Pui Chuen Hui, Eleftherios I. Paschalis, Andrea Cruzat, Pablo Argüeso, James Chodosh, Claes H. Dohlman and Miguel Gonzalez-Andrades are, or were in the past, full-time employees of Massachusetts Eye and Ear Infirmary, Boston – the manufacturer of the Boston Keratoprosthesis.
The datasets generated during and/or analyzed during the current study are available from the corresponding author on reasonable request.

8. REFERENCES

World Health Organization (WHO). Prevention of Blindness and Visual Impairment.

1891 ARTIFICIAL CORNEA *The Lancet* **138** 886

1990 *IAEA: Good radiation practice (GRP). In: IAEA (ed) Guidelines for industrial radiation sterilization of disposable medical products (cobalt-60 gamma irradiation). IAEA, Vienna, Austria.*

Allan J S 1996 Xenotransplantation at a crossroads: prevention versus progress *Nat Med* **2** 18-21

Araki-Sasaki K, Ohashi Y, Sasabe T, Hayashi K, Watanabe H, Tano Y and Handa H 1995 An SV40-immortalized human corneal epithelial cell line and its characterization *Invest Ophthalmol Vis Sci* **36** 614-21

Badylak S F 2004 Xenogeneic extracellular matrix as a scaffold for tissue reconstruction *Transplant immunology* **12** 367-77

Bailey A J, Rhodes D N and Cater C W 1964 Irradiation-Induced Crosslinking of Collagen *Radiation Research* **22** 606-21

Bastian F, Stelzmuller M E, Kratochwill K, Kasimir M T, Simon P and Weigel G 2008 IgG deposition and activation of the classical complement pathway involvement in the activation of human granulocytes by decellularized porcine heart valve tissue *Biomaterials* **29** 1824-32

Bergseth G, Ludviksen J K, Kirschfink M, Giclas P C, Nilsson B and Mollnes T E 2013 An international serum standard for application in assays to detect human complement activation products *Molecular immunology* **56** 232-9

Blusch J H, Patience C and Martin U 2002 Pig endogenous retroviruses and xenotransplantation *Xenotransplantation* **9** 242-51

Boneva R S, Folks T M and Chapman L E 2001 Infectious disease issues in xenotransplantation *Clin Microbiol Rev* **14** 1-14

Bora N S, Gobleman C L, Atkinson J P, Pepose J S and Kaplan H J 1993 Differential expression of the complement regulatory proteins in the human eye *Invest Ophthalmol Vis Sci* **34** 3579-84

Brunette I, Roberts C J, Vidal F, Harissi-Dagher M, Lachaine J, Sheardown H, Durr G M, Proulx S and Griffith M 2017 Alternatives to eye bank native tissue for corneal stromal replacement *Progress in Retinal and Eye Research* **59** 97-130

Cheung D T, Perelman N, Tong D and Nimni M E 1990 The effect of γ-irradiation on collagen molecules, isolated α-chains, and crosslinked native fibers *Journal of Biomedical Materials Research* **24** 581-9

Choi H J, Kim M K, Lee H J, Ko J H, Jeong S H, Lee J I, Oh B C, Kang H J and Wee W R 2011 Efficacy of pig-to-rhesus lamellar corneal xenotransplantation *Invest Ophthalmol Vis Sci* **52** 6643-50

Choi H J, Lee J J, Kim D H, Kim M K, Lee H J, Ko A Y, Kang H J, Park C and Wee W R 2015 Blockade of CD40-CD154 costimulatory pathway promotes long-term survival of full-thickness porcine corneal grafts in nonhuman primates: clinically applicable xenocorneal transplantation *Am J Transplant* **15** 628-41

Cooper D K, Gollackner B and Sachs D H 2002 Will the pig solve the transplantation backlog? *Annu Rev Med* **53** 133-47

Cooper D K, Good A H, Koren E, Oriol R, Malcolm A J, Ippolito R M, Neethling F A, Ye Y, Romano E and Zuhdi N 1993 Identification of alpha-galactosyl and other carbohydrate epitopes that are bound by human anti-pig antibodies: relevance to discordant xenografting in man *Transpl Immunol* **1** 198-205

Cruzat A, Tauber A, Shukla A, Paschalis E I, Pineda R and Dohlman C H 2013 Low-cost and readily available tissue carriers for the Boston keratoprosthesis: a review of possibilities *J Ophthalmol* **2013** 686587

Daoud Y J, Smith R, Smith T, Akpek E K, Ward D E and Stark W J 2011 The intraoperative impression and postoperative outcomes of gamma-irradiated corneas in corneal and glaucoma patch surgery *Cornea* **30** 1387-91

De Ocampo G, Sunga R and De La Cruz-Estrella C 1959 The use of chicken and monkey cornea for human corneal grafting *Acta Med Philipp* **16** 55-64

Du L, Wu X, Pang K and Yang Y 2011 Histological evaluation and biomechanical characterisation of an acellular porcine cornea scaffold *Br J Ophthalmol* **95** 410-4

Durrani K M, Kirmani T H, Hassan M M, Rizvi S M, Tanner J C and Vandeput J J 1974 Penetrating keratoplasty with purified bovine collagen: report of a coordinated trial on fifteen human cases *Ann Ophthalmol* **6** 639-46

Fadlallah A, Atallah M, Cherfan G, Awwad S T, Syed Z A and Melki S A 2014 Gamma-irradiated corneas as carriers for the Boston type 1 keratoprosthesis: advantages and outcomes in a surgical mission setting *Cornea* **33** 235-9

Fagerholm P, Lagali N S, Merrett K, Jackson W B, Munger R, Liu Y, Polarek J W, Soderqvist M and Griffith M 2010 A biosynthetic alternative to human donor tissue for inducing corneal regeneration: 24-month follow-up of a phase 1 clinical study *Sci Transl Med* **2** 46ra61

Gain P, Jullienne R, He Z, Aldossary M, Acquart S, Cognasse F and Thuret G 2016 Global Survey of Corneal Transplantation and Eye Banking *JAMA Ophthalmol* **134** 167-73

Gipson I K, Spurr-Michaud S, Argueso P, Tisdale A, Ng T F and Russo C L 2003 Mucin gene expression in immortalized human corneal-limbal and conjunctival epithelial cell lines *Invest Ophthalmol Vis Sci* **44** 2496-506

Gipson I K, Spurr-Michaud S, Tisdale A and Menon B B 2014 Comparison of the transmembrane mucins MUC1 and MUC16 in epithelial barrier function *PLoS One* **9** e100393

Gipson I K, Spurr-Michaud S J and Tisdale A S 1987 Anchoring fibrils form a complex network in human and rabbit cornea *Invest Ophthalmol Vis Sci* **28** 212-20

Gonzalez-Andrades M, Alonso-Pastor L, Mauris J, Cruzat A, Dohlman C H and Argueso P 2016 Establishment of a novel in vitro model of stratified epithelial wound healing with barrier function *Sci Rep* **6** 19395

Gonzalez-Andrades M, Carriel V, Rivera-Izquierdo M, Garzon I, Gonzalez-Andrades E, Medialdea S, Alaminos M and Campos A 2015 Effects of Detergent-Based Protocols on Decellularization of Corneas With Sclerocorneal Limbus. Evaluation of Regional Differences *Transl Vis Sci Technol* **4** 13

Gonzalez-Andrades M, de la Cruz Cardona J, Ionescu A M, Campos A, Del Mar Perez M and Alaminos M 2011 Generation of bioengineered corneas with decellularized xenografts and human keratocytes *Invest Ophthalmol Vis Sci* **52** 215-22

Gonzalez-Andrades M, Sharifi R, Islam M M, Divoux T, Haist M, Paschalis E I, Gelfand L, Mamodaly S, Di Cecilia L, Cruzat A, Ulm F J, Chodosh J, Delori F and Dohlman C H 2018 Improving the practicality and safety of artificial corneas: Pre-assembly and gamma-rays sterilization of the Boston Keratoprosthesis *Ocul Surf* **16** 322-30

Gorham S D, Srivastava S, French D A and Scott R 1993 The effect of gamma-ray and ethylene oxide sterilization on collagen-based wound-repair materials *Journal of Materials Science: Materials in Medicine* **4** 40-9

Gotzinger E, Pircher M, Sticker M, Fercher A F and Hitzenberger C K 2004 Measurement and imaging of birefringent properties of the human cornea with phase-resolved, polarization-sensitive optical coherence tomography *J Biomed Opt* **9** 94-102

Groth C G 2007 The potential advantages of transplanting organs from pig to man: A transplant Surgeon's view *Indian J Urol* **23** 305-9

Hackett J M, Ferguson C, Dare E, McLaughlin C R and Griffith M 2010 Optimal neural differentiation and extension of hybrid neuroblastoma cells (NDC) for nerve-target evaluations using a multifactorial approach *Toxicol In Vitro* **24** 567-77

Haq M 1972 Fish cornea for grafting *British medical journal* **2** 712-3

Hara H and Cooper D K 2011 Xenotransplantation--the future of corneal transplantation? *Cornea* **30** 371-8

Hara H, Long C, Lin Y J, Tai H C, Ezzelarab M, Ayares D and Cooper D K 2008 In vitro investigation of pig cells for resistance to human antibody-mediated rejection *Transpl Int* **21** 1163-74

Hashimoto Y, Funamoto S, Sasaki S, Negishi J, Honda T, Hattori S, Nam K, Kimura T, Mochizuki M, Kobayashi H and Kishida A 2015 Corneal Regeneration by Deep Anterior Lamellar Keratoplasty (DALK) Using Decellularized Corneal Matrix *PLOS ONE* **10** e0131989

Hee M R, Huang D, Swanson E A and Fujimoto J G 1992 Polarization-sensitive low-coherence reflectometer for birefringence characterization and ranging *J. Opt. Soc. Am. B* **9** 903-8

Huai G, Qi P, Yang H and Wang Y 2016 Characteristics of alpha-Gal epitope, anti-Gal antibody, alpha1,3 galactosyltransferase and its clinical exploitation (Review) *Int J Mol Med* **37** 11-20

Huang Y H, Tseng F W, Chang W H, Peng I C, Hsieh D J, Wu S W and Yeh M L 2017 Preparation of acellular scaffold for corneal tissue engineering by supercritical carbon dioxide extraction technology *Acta Biomater* **58** 238-43

Irie A, Koyama S, Kozutsumi Y, Kawasaki T and Suzuki A 1998 The molecular basis for the absence of N-glycolylneuraminic acid in humans *J Biol Chem* **273** 15866-71

Islam M M, Ravichandran R, Olsen D, Ljunggren M K, Fagerholm P, Lee C J, Griffith M and Phopase J 2016 Self-assembled collagen-like-peptide implants as alternatives to human donor corneal transplantation *RSC Advances* **6** 55745-9

Ju C, Gao L, Wu X and Pang K 2012 A human corneal endothelium equivalent constructed with acellular porcine corneal matrix *Indian J Med Res* **135** 887-94

Kim M K and Hara H 2015 Current status of corneal xenotransplantation *Int J Surg* **23** 255-60

Kim Y G, Oh J Y, Gil G C, Kim M K, Ko J H, Lee S, Lee H J, Wee W R and Kim B G 2009 Identification of alpha-Gal and non-Gal epitopes in pig corneal endothelial cells and keratocytes by using mass spectrometry *Curr Eye Res* **34** 877-95

Kiritoshi A, SundarRaj N and Thoft R A 1991 Differentiation in cultured limbal epithelium as defined by keratin expression *Invest Ophthalmol Vis Sci* **32** 3073-7

Kissam R S 1844 Ceratoplastice in man *New York Medical Journal* **2** 281-
Koh L B, Islam M M, Mitra D, Noel C W, Merrett K, Odorcic S, Fagerholm P, Jackson W B, Liedberg B, Phopase J and Griffith M 2013 Epoxy cross-linked collagen and collagen-laminin Peptide hydrogels as corneal substitutes *J Funct Biomater* **4** 162-77
Lai Y S, Chen W C, Huang C H, Cheng C K, Chan K K and Chang T K 2015 The effect of graft strength on knee laxity and graft in-situ forces after posterior cruciate ligament reconstruction *PLoS One* **10** e0127293
Larkin D F and Williams K A 1995 The host response in experimental corneal xenotransplantation *Eye* **9 (Pt 2)** 254-60
Lee H I, Kim M K, Ko J H, Lee H J, Lee J H and Wee W R 2006 The Characteristics of Porcine Cornea as a Xenograft *Journal of the Korean ophthalmological society* **47** 2020-9
Lee H I, Kim M K, Oh J Y, Ko J H, Lee H J, Wee W R and Lee J H 2007 Gal alpha(1-3)Gal expression of the cornea in vitro, in vivo and in xenotransplantation *Xenotransplantation* **14** 612-8
Lee W, Miyagawa Y, Long C, Ekser B, Walters E, Ramsoondar J, Ayares D, Tector A J, Cooper D K and Hara H 2016 Expression of NeuGc on Pig Corneas and Its Potential Significance in Pig Corneal Xenotransplantation *Cornea* **35** 105-13
Leontiou I, Matthopoulos D P, Tzaphlidou M and Glaros D 1993 The effect of gamma irradiation on collagen fibril structure *Micron* **24** 13-6
Lin Y, Zheng Q, Hua S, Meng Y, Chen W and Wang Y 2017 Cross-linked decellularized porcine corneal graft for treating fungal keratitis *Sci Rep* **7** 9955
Liu W, Merrett K, Griffith M, Fagerholm P, Dravida S, Heyne B, Scaiano J C, Watsky M A, Shinozaki N, Lagali N, Munger R and Li F 2008 Recombinant human collagen for tissue engineered corneal substitutes *Biomaterials* **29** 1147-58
Lo W C, Villiger M, Golberg A, Broelsch G F, Khan S, Lian C G, Austen W G, Jr., Yarmush M and Bouma B E 2016 Longitudinal, 3D Imaging of Collagen Remodeling in Murine Hypertrophic Scars In Vivo Using Polarization-Sensitive Optical Frequency Domain Imaging *J Invest Dermatol* **136** 84-92
Lynch A P and Ahearne M 2013 Strategies for developing decellularized corneal scaffolds *Exp Eye Res* **108** 42-7
McCarey B E and Schmidt F H 1990 Modeling glucose distribution in the cornea *Curr Eye Res* **9** 1025-39
Mendoza-Novelo B, Avila E E, Cauich-Rodriguez J V, Jorge-Herrero E, Rojo F J, Guinea G V and Mata-Mata J L 2011 Decellularization of pericardial tissue and its impact on tensile viscoelasticity and glycosaminoglycan content *Acta Biomater* **7** 1241-8
Merrett K, Liu W, Mitra D, Camm K D, McLaughlin C R, Liu Y, Watsky M A, Li F, Griffith M and Fogg D E 2009 Synthetic neoglycopolymer-recombinant human collagen hybrids as biomimetic crosslinking agents in corneal tissue engineering *Biomaterials* **30** 5403-8
Miekka S I, Forng R Y, Rohwer R G, MacAuley C, Stafford R E, Flack S L, MacPhee M, Kent R S and Drohan W N 2003 Inactivation of viral and prion pathogens by γ-irradiation under conditions that maintain the integrity of human albumin *Vox Sanguinis* **84** 36-44
Mirazul Islam M, Cėpla V, He C, Edin J, Rakickas T, Kobuch K, Ruželė Ž, Bruce Jackson W, Rafat M, Lohmann C P, Valiokas R and Griffith M 2015 Functional fabrication of recombinant human collagen–phosphorylcholine hydrogels for regenerative medicine applications *Acta Biomaterialia* **12** 70-80

Mollnes T E, Brekke O L, Fung M, Fure H, Christiansen D, Bergseth G, Videm V, Lappegard K T, Kohl J and Lambris J D 2002 Essential role of the C5a receptor in E coli-induced oxidative burst and phagocytosis revealed by a novel lepirudin-based human whole blood model of inflammation *Blood* **100** 1869-77

Myung D, Derr K, Huie P, Noolandi J, Ta K P and Ta C N 2006 Glucose permeability of human, bovine, and porcine corneas in vitro *Ophthalmic Res* **38** 158-63

Nara S, Chameettachal S, Midha S, Singh H, Tandon R, Mohanty S and Ghosh S 2015 Strategies for faster detachment of corneal cell sheet using micropatterned thermoresponsive matrices *Journal of Materials Chemistry B* **3** 4155-69

Newman K D, McLaughlin C R, Carlsson D, Li F, Liu Y and Griffith M 2006 Bioactive hydrogel-filament scaffolds for nerve repair and regeneration *Int J Artif Organs* **29** 1082-91

O'Day D M 1989 Diseases potentially transmitted through corneal transplantation *Ophthalmology* **96** 1133-7; discussion 7-8

O'Rahilly R and Meyer D B 1960 The periodic acid-Schiffreaction in the cornea of the developing chick *Z Anat Entwicklungsgesch* **121** 351-68

Oliva M S, Schottman T and Gulati M 2012 Turning the tide of corneal blindness *Indian J Ophthalmol* **60** 423-7

Padler-Karavani V and Varki A 2011 Potential impact of the non-human sialic acid N-glycolylneuraminic acid on transplant rejection risk *Xenotransplantation* **18** 1-5

Panda A, Vanathi M, Kumar A, Dash Y and Priya S 2007 Corneal graft rejection *Surv Ophthalmol* **52** 375-96

Pang K, Du L and Wu X 2010 A rabbit anterior cornea replacement derived from acellular porcine cornea matrix, epithelial cells and keratocytes *Biomaterials* **31** 7257-65

Polisetti N, Islam M M and Griffith M 2013 The artificial cornea *Methods Mol Biol* **1014** 45-52

Rafat M, Li F, Fagerholm P, Lagali N S, Watsky M A, Munger R, Matsuura T and Griffith M 2008 PEG-stabilized carbodiimide crosslinked collagen-chitosan hydrogels for corneal tissue engineering *Biomaterials* **29** 3960-72

Sandrin M S and McKenzie I F 1994 Gal alpha (1,3)Gal, the major xenoantigen(s) recognised in pigs by human natural antibodies *Immunol Rev* **141** 169-90

Sasaki S, Funamoto S, Hashimoto Y, Kimura T, Honda T, Hattori S, Kobayashi H, Kishida A and Mochizuki M 2009 In vivo evaluation of a novel scaffold for artificial corneas prepared by using ultrahigh hydrostatic pressure to decellularize porcine corneas *Mol Vis* **15** 2022-8

Schermer A, Galvin S and Sun T T 1986 Differentiation-related expression of a major 64K corneal keratin in vivo and in culture suggests limbal location of corneal epithelial stem cells *J Cell Biol* **103** 49-62

Seifert P 2017 Modified Hiraoka TEM grid staining apparatus and technique using 3D printed materials and gadolinium triacetate tetrahydrate, a nonradioactive uranyl acetate substitute *Journal of Histotechnology* **40** 130-5

Shafiq M A, Gemeinhart R A, Yue B Y and Djalilian A R 2012 Decellularized human cornea for reconstructing the corneal epithelium and anterior stroma *Tissue Eng Part C Methods* **18** 340-8

Shi Y, Bikkuzin T, Song Z, Jin X, Jin H, Li X and Zhang H 2017 Comprehensive evaluation of decellularized porcine corneal after clinical transplantation *Xenotransplantation* **24**

Shirai K, Okada Y, Cheon D J, Miyajima M, Behringer R R, Yamanaka O and Saika S 2014 Effects of the loss of conjunctival Muc16 on corneal epithelium and stroma in mice *Invest Ophthalmol Vis Sci* **55** 3626-37

Singh R, Singh D and Singh A 2016 Radiation sterilization of tissue allografts: A review *World J Radiol* **8** 355-69

Soomsawasdi B R N, Bhadrakom S. 1964 Hetero-keratoplasy using gibbon donor corneae *Asia Pacific Academy of Ophthalmology* **2** 251-61

Stevenson W, Cheng S F, Emami-Naeini P, Hua J, Paschalis E I, Dana R and Saban D R 2012 Gamma-irradiation reduces the allogenicity of donor corneas *Invest Ophthalmol Vis Sci* **53** 7151-8

Sweeney D F, Xie R Z, O'Leary D J, Vannas A, Odell R, Schindhelm K, Cheng H Y, Steele J G and Holden B A 1998 Nutritional requirements of the corneal epithelium and anterior stroma: clinical findings *Invest Ophthalmol Vis Sci* **39** 284-91

Todani A, Ciolino J B, Ament J D, Colby K A, Pineda R, Belin M W, Aquavella J V, Chodosh J and Dohlman C H 2011 Titanium back plate for a PMMA keratoprosthesis: clinical outcomes *Graefes Arch Clin Exp Ophthalmol* **249** 1515-8

Tzaphlidou M, Leontiou I and Glaros D 1991 The effect of gamma irradiation on the organization of mouse skin collagen fibrils. The positive staining pattern *Micron and Microscopica Acta* **22** 207-12

Vail A, Gore S M, Bradley B A, Easty D L, Rogers C A and Armitate W J 1996 Clinical and surgical factors influencing corneal graft survival, visual acuity, and astigmatism. Corneal Transplant Follow-up Study Collaborators *Ophthalmology* **103** 41-9

Villiger M, Otsuka K, Karanasos A, Doradla P, Ren J, Lippok N, Shishkov M, Daemen J, Diletti R, van Geuns R J, Zijlstra F, van Soest G, Libby P, Regar E, Nadkarni S K and Bouma B E 2017 Coronary Plaque Microstructure and Composition Modify Optical Polarization: A New Endogenous Contrast Mechanism for Optical Frequency Domain Imaging *JACC Cardiovasc Imaging*

Villiger M, Zhang E Z, Nadkarni S K, Oh W Y, Vakoc B J and Bouma B E 2013 Spectral binning for mitigation of polarization mode dispersion artifacts in catheter-based optical frequency domain imaging *Opt Express* **21** 16353-69

Watsky M A, Jablonski M M and Edelhauser H F 1988 Comparison of conjunctival and corneal surface areas in rabbit and human *Curr Eye Res* **7** 483-6

Wee S W, Choi S U and Kim J C 2015 Deep anterior lamellar keratoplasty using irradiated acellular cornea with amniotic membrane transplantation for intractable ocular surface diseases *Korean J Ophthalmol* **29** 79-85

Wong K H, Kam K W, Chen L J and Young A L 2017 Corneal blindness and current major treatment concern-graft scarcity *Int J Ophthalmol* **10** 1154-62

Wood J N, Bevan S J, Coote P R, Dunn P M, Harmar A, Hogan P, Latchman D S, Morrison C, Rougon G, Theveniau M and et al. 1990 Novel cell lines display properties of nociceptive sensory neurons *Proc Biol Sci* **241** 187-94

Yoeruek E, Bayyoud T, Maurus C, Hofmann J, Spitzer M S, Bartz-Schmidt K U and Szurman P 2012a Decellularization of porcine corneas and repopulation with human corneal cells for tissue-engineered xenografts *Acta Ophthalmol* **90** e125-31

Yoeruek E, Bayyoud T, Maurus C, Hofmann J, Spitzer M S, Bartz-Schmidt K U and Szurman P 2012b Reconstruction of corneal stroma with decellularized porcine xenografts in a rabbit model *Acta Ophthalmol* **90** e206-10

Yoshida J, Heflin T, Zambrano A, Pan Q, Meng H, Wang J, Stark W J and Daoud Y J 2015 Gamma-Irradiated Sterile Cornea for Use in Corneal Transplants in a Rabbit Model *Middle East Afr J Ophthalmol* **22** 346-51

Yuan C, Bothun E D, Hardten D R, Tolar J and McLoon L K 2016 A novel explanation of corneal clouding in a bone marrow transplant-treated patient with Hurler syndrome *Exp Eye Res* **148** 83-9

Zhang M C, Liu X, Jin Y, Jiang D L, Wei X S and Xie H T 2015 Lamellar keratoplasty treatment of fungal corneal ulcers with acellular porcine corneal stroma *Am J Transplant* **15** 1068-75

Zhu A and Hurst R 2002 Anti-N-glycolylneuraminic acid antibodies identified in healthy human serum *Xenotransplantation* **9** 376-81